

# Lake heatwaves under climate change

<https://doi.org/10.1038/s41586-020-03119-1>

Received: 15 April 2020

Accepted: 21 October 2020

Published online: 20 January 2021

 Check for updates

R. Iestyn Woolway<sup>1,2</sup>✉, Eleanor Jennings<sup>1</sup>, Tom Shatwell<sup>3</sup>, Malgorzata Golub<sup>4</sup>, Don C. Pierson<sup>4</sup> & Stephen C. Maberly<sup>5</sup>

Lake ecosystems, and the organisms that live within them, are vulnerable to temperature change<sup>1–5</sup>, including the increased occurrence of thermal extremes<sup>6</sup>. However, very little is known about lake heatwaves—periods of extreme warm lake surface water temperature—and how they may change under global warming. Here we use satellite observations and a numerical model to investigate changes in lake heatwaves for hundreds of lakes worldwide from 1901 to 2099. We show that lake heatwaves will become hotter and longer by the end of the twenty-first century. For the high-greenhouse-gas-emission scenario (Representative Concentration Pathway (RCP) 8.5), the average intensity of lake heatwaves, defined relative to the historical period (1970 to 1999), will increase from  $3.7 \pm 0.1$  to  $5.4 \pm 0.8$  degrees Celsius and their average duration will increase dramatically from  $7.7 \pm 0.4$  to  $95.5 \pm 35.3$  days. In the low-greenhouse-gas-emission RCP 2.6 scenario, heatwave intensity and duration will increase to  $4.0 \pm 0.2$  degrees Celsius and  $27.0 \pm 7.6$  days, respectively. Surface heatwaves are longer-lasting but less intense in deeper lakes (up to 60 metres deep) than in shallower lakes during both historic and future periods. As lakes warm during the twenty-first century<sup>7,8</sup>, their heatwaves will begin to extend across multiple seasons, with some lakes reaching a permanent heatwave state. Lake heatwaves are likely to exacerbate the adverse effects of long-term warming in lakes and exert widespread influence on their physical structure and chemical properties. Lake heatwaves could alter species composition by pushing aquatic species and ecosystems to the limits of their resilience. This in turn could threaten lake biodiversity<sup>9</sup> and the key ecological and economic benefits that lakes provide to society.

There is compelling evidence that climate change is leading to more frequent and more intense heatwaves over land<sup>10,11</sup> and at the surface of the ocean<sup>12–16</sup>, increasing the risk of severe and in some cases irreversible ecological and socioeconomic impacts<sup>17</sup>. In comparison, we know much less about heatwaves in lakes and how they will change within a warming world. This knowledge gap is of considerable concern given the high vulnerability of lakes to thermal extremes, and the ecosystem goods and services that they provide<sup>6,18</sup>.

A lake heatwave event can be defined, similar to marine heatwaves<sup>13,17,19</sup>, as a period in which lake surface temperatures exceed a local and seasonally varying 90th percentile threshold, relative to a baseline climatological mean (the average temperature for the day or month of year evaluated over the base period), for at least five days (Methods; Extended Data Fig. 1a). Here, we quantify past changes and assess future ones for different lake heatwave characteristics using a lake model forced with atmospheric data (air temperature, solar and thermal radiation, wind speed, atmospheric pressure and humidity) from an ensemble of four bias-corrected twentieth and twenty-first century climate projections (Methods). Specifically, using satellite-derived lake surface temperatures to optimize key parameters of a lake model (that is, to represent the thermal dynamics of the individual lakes), we

simulate daily temperatures for hundreds of lakes worldwide (Extended Data Fig. 2a–c), and investigate how lake heatwave intensity and duration respond to climate change. The ability of the optimized lake model to simulate lake heatwaves is evaluated by comparing the simulations with satellite-derived lake temperatures during the historic period (see Methods). Good agreement was obtained between simulations and observations of lake heatwaves and also of mean lake surface temperatures (Extended Data Fig. 3). Using the optimized model, we simulated daily lake surface temperatures for all of the studied lakes from 1901 to 2099. Historical simulations used anthropogenic greenhouse gas and aerosol forcing in addition to natural forcing, and cover the period 1901 to 2005. Future projections, which represent the evolution of the climate system subject to three different anthropogenic greenhouse gas emission scenarios covering the period 2006 to 2099, RCP 2.6 (the low-emission scenario), 6.0 (the medium-emission scenario), and 8.5 (the high-emission scenario), are also investigated. For all model experiments, the climatological mean used to define anomalies was calculated relative to a 30-year base period (1970 to 1999).

Simulated lake heatwave events from 1901 to 2099 are summarized to produce a set of characteristics for lake heatwaves. We derived metrics for duration (time between start and end dates of a lake heatwave event)

<sup>1</sup>Centre for Freshwater and Environmental Studies, Dundalk Institute of Technology, Dundalk, Ireland. <sup>2</sup>European Space Agency Climate Office, ECSAT, Didcot, UK. <sup>3</sup>Department of Lake Research, Helmholtz Centre for Environmental Research (UFZ), Magdeburg, Germany. <sup>4</sup>Department of Ecology and Genetics/Limnology, Uppsala University, Uppsala, Sweden. <sup>5</sup>UK Centre for Ecology and Hydrology, Lancaster Environment Centre, Lancaster, UK. ✉e-mail: riwoolway@gmail.com

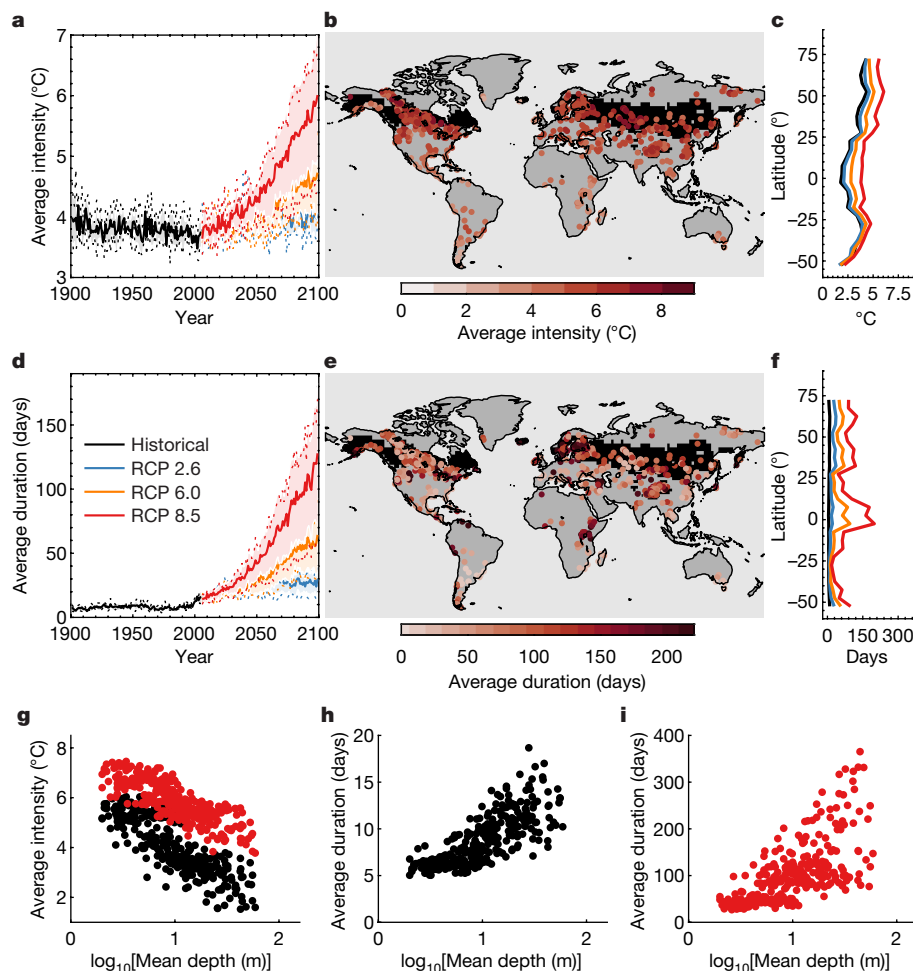


**Fig. 1 | Historical and future projections of the intensity and duration of lake heatwaves.** Temporal and spatial patterns in the average intensity (a–c) and duration (d–f) of lake heatwaves. **a, d**, Lake heatwaves under climate change. The temporal changes in lake heatwaves from 1901 to 2099 under historical and future climate forcing (RCP 2.6, 6.0, 8.5). The thick lines show the mean across all studied lakes, the shaded regions represent the standard deviation, and the dashed lines represent the range across the lake-climate model ensembles. **b, e**, Future (2070–2099) lake heatwaves under RCP 8.5. The average intensity and duration of lake heatwaves in each lake by the end of the

twenty-first century (averaged for all years from 2070 to 2099) under RCP 8.5. **c, f**, Latitudinal averages (5° bins) of the lake heatwave metrics under historical (1970–1999) and future (2070–2099) forcing. **g–i**, The relationship between lake heatwaves and average lake depth ( $\log_{10}$ ), under historic (black) and future (red; RCP 8.5) forcing for lakes situated in the Northern Cool thermal region (shown as black regions in panels **b** and **e**; relationships for other thermal regions are shown in Extended Data Figs. 4–6). All results are based on the average simulations from the lake model driven by the four climate models.

and intensity (mean temperature anomaly over the heatwave). We also use an intensity-based lake heatwave category to define the relative strength of each lake heatwave (see, for example, Extended Data Fig. 1b), where each event is classed as being Moderate, Strong, Severe or Extreme, following the definitions of ref. <sup>20</sup>. These categories are defined by the maximum intensity of each lake heatwave event scaled by the threshold temperature anomaly exceeding the climatological mean. The Moderate category is defined as the time in which the lake surface temperature is above the 90th percentile of the climatological distribution; the Strong category means that the largest temperature anomaly during the event is more than twice as large as the difference between the seasonal average and the 90th percentile; the Severe category means that the largest anomaly is more than three times the difference between the seasonal average and the 90th percentile; and the Extreme category means that the largest anomaly is four or more times the difference between the seasonal average and the 90th percentile. We calculated time series of the annual average intensity and average duration of lake heatwave events, as well as the total number of lake heatwave days within a year, and the number of days belonging to each of the defined lake heatwave categories. The season of lake heatwave occurrence was also investigated.

Our global lake temperature simulations suggest that a typical lake heatwave event, averaged for all years from 1970 to 1999, had an average intensity of  $3.7 \pm 0.1$  °C and lasted, on average,  $7.7 \pm 0.4$  days (quoted uncertainties represent the standard deviation from the lake model driven by the four climate model projections). Lake heatwave intensity and duration vary depending on the climate model projection used with a range of 0.1 °C and 0.8 days, respectively, across the lake-climate model ensembles (that is, the difference between the minimum and maximum of the simulations). Hereafter, for each lake heatwave metric quoted, we also provide the minimum and maximum from the four climate model ensembles (that is, [min, max]). During the twenty-first century, lake heatwave intensity and duration was projected to increase considerably worldwide (Fig. 1). Some lakes have already experienced noticeable change in recent decades (Extended Data Fig. 1c–f). The magnitude of change of these lake heatwave metrics during the twenty-first century increases with the severity of the RCP scenario. For the low-emission scenario, the average intensity of lake heatwaves, averaged for all years from 2070 to 2099, will increase to  $4.0 \pm 0.2$  [3.7, 4.2] °C and the average duration will increase threefold to  $27.0 \pm 7.6$  days [16.1, 33.7]. Under the high-emission scenario, the

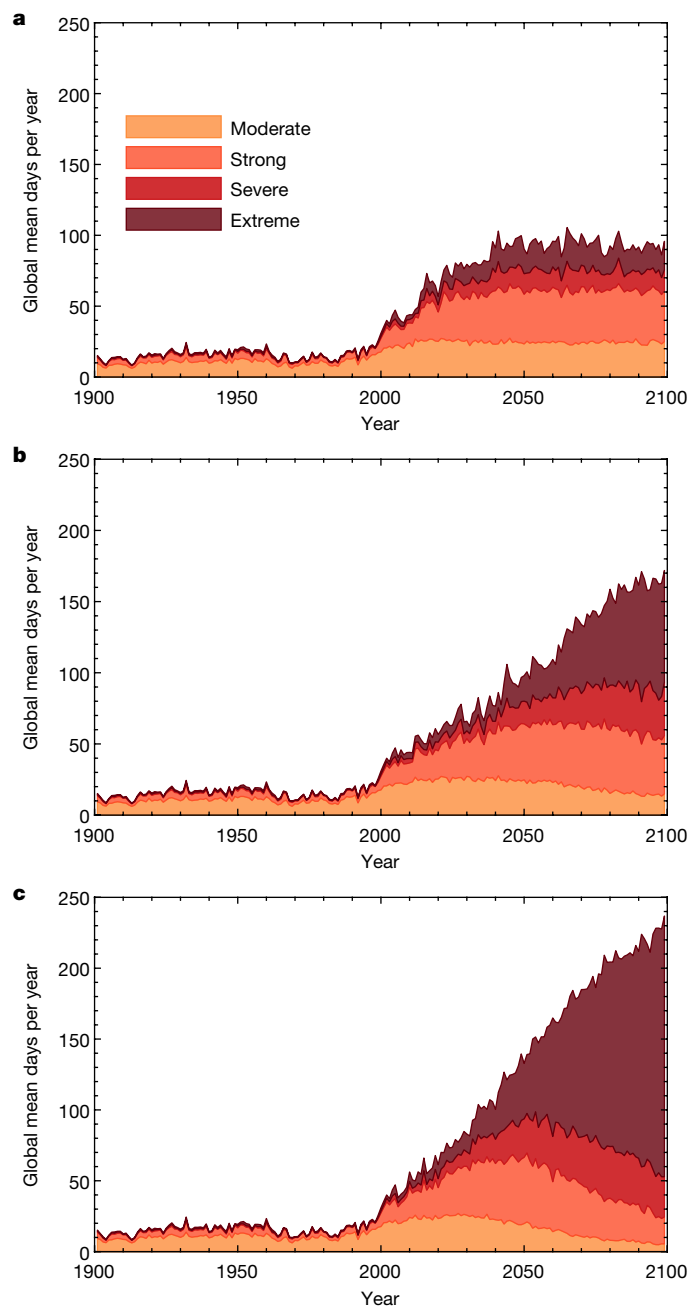


**Fig. 2 | Historical and future projections of global lake heatwave strength.** Time series of the global annual mean count of Moderate (light orange), Strong (orange), Severe (red), and Extreme (dark red) simulated lake heatwave days under historical and future climate forcing. Future projections are subject to three different greenhouse gas emission scenarios: **a**, RCP 2.6; **b**, RCP 6.0; and **c**, RCP 8.5. The total stacked amount in each panel is equivalent to the total lake heatwave days under that particular forcing scenario. All results are based on the average simulations from the lake model driven by the four climate models.

intensity and duration of lake heatwaves will be much greater by the end of the twenty-first century. The average intensity of lake heatwaves will increase to  $5.4 \pm 0.8$  [4.3, 6.1] °C, and the average duration of lake heatwaves will increase 12-fold to  $95.5 \pm 35.3$  [45.8, 125.6] days (Fig. 1). Similar to marine heatwaves<sup>12,13</sup>, the intensity of lake heatwaves is linked to temperature variability. It is higher in regions with high surface temperature variability such as high-latitude lakes<sup>8</sup>, and lower in regions with low variability, such as in tropical lakes (Fig. 1c). However, the projected lake heatwave events at higher latitudes tended to be relatively

short-lived compared to those experienced in low-latitude lakes, in particular under future climate change (Fig. 1f).

Our simulations also showed a dependence of the average intensity and duration of heatwave events on average lake depth ( $\log_{10}$  transformed) (Fig. 1g–i). To investigate this depth dependence further, we first separated the studied lakes according to the thermal regions in which they reside. Following the definitions of ref. <sup>8</sup>, we separated the studied lakes into nine thermal regions, which are categorized according to their seasonal patterns of surface temperature (Extended Data Fig. 2d–g). Given the preponderance of lakes in high northern latitudes<sup>21</sup> (Extended Data Fig. 2g), over 70% of our studied lakes are situated within the three northernmost thermal regions: Northern Frigid ( $n = 87$ ), Northern Cool ( $n = 313$ ) and Northern Temperate ( $n = 123$ ). Within each of the nine thermal regions, we calculated the relationship between lake depth and the intensity and duration of lake heatwaves (Extended Data Figs. 4–6). For lakes situated in the Northern Cool region, where the majority of the studied lakes are located, we calculated a statistically significant ( $P < 0.001$ ) relationship between lake depth and lake heatwave intensity ( $R_{\text{adj}}^2 = 0.72$ ) and duration ( $R_{\text{adj}}^2 = 0.42$ ) under RCP 8.5 (Fig. 1g–i). Similar relationships were also observed under different climate trajectories as well as within the other thermal regions with a sufficient number of lakes to make such comparisons (Extended Data Figs. 4–6). Overall, we find that deeper lakes experience less intense but longer-lasting lake heatwaves. This depth effect is primarily because surface temperature anomalies in deep lakes, owing to their large thermal inertia, are (i) less sensitive to day-to-day changes in atmospheric forcing and short-term climatic extremes and (ii) surface thermal anomalies are eroded more slowly<sup>22,23</sup>. Additional lake-specific factors, such as the surrounding topography and mixing regimes, as well as temporal variations in these lake attributes and over-lake meteorology (for example, wind speed), can also be important influences on heatwaves in lakes. However, our analysis suggests that lake depth explains a large proportion of the variability in lake heatwaves within each lake thermal region.

The RCP scenario had a strong influence on the projected intensity of events and therefore the exposure to the most extreme lake heatwaves during the twenty-first century (Fig. 2). During, and particularly towards the latter stages of the twentieth century (averaged for all years from 1970 to 1999), the majority of lake heatwave events worldwide were categorized as Moderate ( $70 \pm 3.2$  [66.5, 73.9]%) with relatively few Strong events ( $22 \pm 2.8$  [19.5, 25.2]%) and very few Severe ( $4 \pm 0.6$  [3.0, 4.4]%) or Extreme ( $4 \pm 0.3$  [3.3, 4.0]%) events. Under the RCP 2.6 scenario, future projections suggest that by the end of the twenty-first century (averaged for all years from 2070 to 2099) there will be a more even partition between the four lake heatwave categories (that is, percentage contributions of Moderate:Strong:Severe:Extreme =  $28 \pm 9.6$  [20.5, 41.9]: $40 \pm 2.2$  [37.3, 42.5]: $14 \pm 3.5$  [9.2, 16.8]: $18 \pm 6.8$  [9.9, 25.4]), indicating an increase in Strong, Severe and Extreme lake heatwaves. Under RCP 8.5, Extreme lake heatwaves were projected to make up the majority of all events ( $65 \pm 17.4\%$ ) by the end of the twenty-first century (Fig. 2), whereas Moderate events were rare ( $4 \pm 3.1\%$ ; percentage contributions of Moderate:Strong:Severe:Extreme =  $4 \pm 3.1$  [1.6, 11.3]: $14 \pm 9.1$  [7.3, 27.7]: $17 \pm 3.9$  [12.1, 21.7]: $65 \pm 17.4$  [39.4, 79.0]).

During the historical period, lake heatwaves were prominent features in lakes during Spring, Summer and/or Autumn with about  $27 \pm 3\%$ , about  $38 \pm 4\%$ , and about  $24 \pm 4\%$ , respectively, of the lakes studied experiencing a lake heatwave event, on average, within a given year. As the climate warms during the twenty-first century, and lake heatwaves become more intense and longer-lasting, the time of year in which they occur will also change (Fig. 3). Specifically, under the high-greenhouse-gas-emission scenario we project that by the end of the twenty-first century, lake heatwaves will no longer be restricted to a single season but will extend across multiple seasons (Fig. 3e–l). Under this scenario,  $35 \pm 3\%$  of the lakes included in our simulations experienced heatwaves that began in Spring and ended in Summer (Fig. 3f),

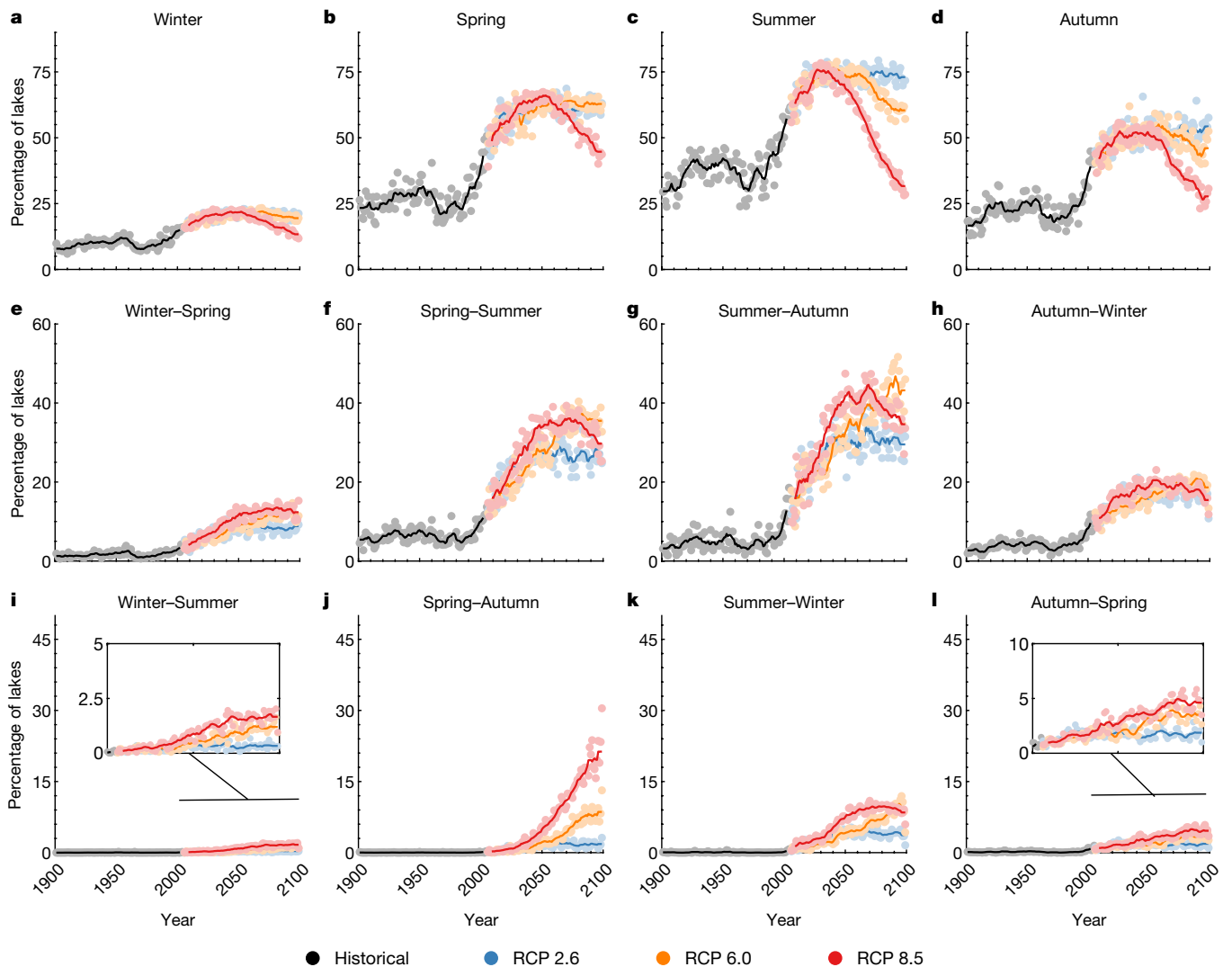


**Fig. 3 | Seasonal variations in lake heatwave occurrence under historical and future climate change.** Temporal changes in the season(s) during which the simulated lake heatwaves occur under historic (1901–2005) and future (2006–2099) climate forcing. Future projections are subject to three different greenhouse gas emission scenarios (RCP 2.6, RCP 6.0 and RCP 8.5). Shown are the percentage of studied lakes which experience a heatwave during a single season (Winter, Spring, Summer, Autumn) only (a–d), and/or experience a heatwave which extended across two (e–h) or three (i–l) seasons. We note that

the axis limits are different in panels a–d, e–h and i–l. Each point represents the percentage of lakes globally during each year, and the solid line represents a 7-year moving average (included for illustration). The decline in panels a–d towards the end of the twenty-first century is due to fewer lakes experiencing heatwaves that are maintained only for a single season. Insets in panels i and l show the same data on an expanded scale. All results are based on the average simulations from the lake model driven by the four climate models. June is used to define the start of boreal summer and December the start of austral summer.

and/or began in Summer and ended in Autumn ( $38 \pm 3\%$ ; Fig. 3g). By the end of the century, more than  $17 \pm 2\%$  of lakes experienced a lake heatwave event that began in Spring and was maintained until Autumn (Fig. 3j).

By the end of the twenty-first century, the total annual duration of lake heatwave days per year, which is typically greater at lower latitudes (Fig. 4b, c) and in deeper lakes (Fig. 4d, e; Extended Data Figs. 7, 8), is projected to increase considerably (Fig. 4a). In particular, under RCP 8.5, the global average total duration of lake heatwave days, averaged for all years from 2070 to 2099, will increase 12-fold to  $219 \pm 44$  [155.1, 254.4] days, compared to  $17 \pm 3$  [14.8, 20.0] days during the historic period (that is, averaged for all years from 1970 to 1999). Some lakes will also reach a permanent lake heatwave state, which we define as when lake surface temperatures exceed the lake heatwave threshold continuously over a full calendar year. The number of studied lakes that will experience a permanent heatwave state will increase during the

twenty-first century, but will differ depending on the RCP scenario considered (Fig. 4e). Under RCP 8.5, over  $80.5 \pm 47$  [18, 124] of the studied lakes will reach a permanent heatwave state by 2099 (Fig. 4f). Seasonal ice cover, which is important for a range of lake ecosystem services as well as the regulation of the hydrological cycle<sup>24</sup>, will influence the number of lakes that experience a permanent heatwave state, because lakes that freeze annually will not experience a heatwave that endures throughout the entire year. For the studied lakes that are projected to be ice-free by 2070–2099, the number of which will increase during the twenty-first century (Extended Data Fig. 9a), we project that approximately half ( $45 \pm 22\%$ ) of these will reach a permanent heatwave state by 2099 under RCP 8.5 (Extended Data Fig. 9b). The influence on lake heatwaves of increasingly ice-free winters is already apparent in Lake Vättern, Sweden<sup>25</sup> (Extended Data Fig. 1c, e).

The emergence of a permanent lake heatwave state implies that extremes in the traditional sense will no longer be ‘extreme’, and that

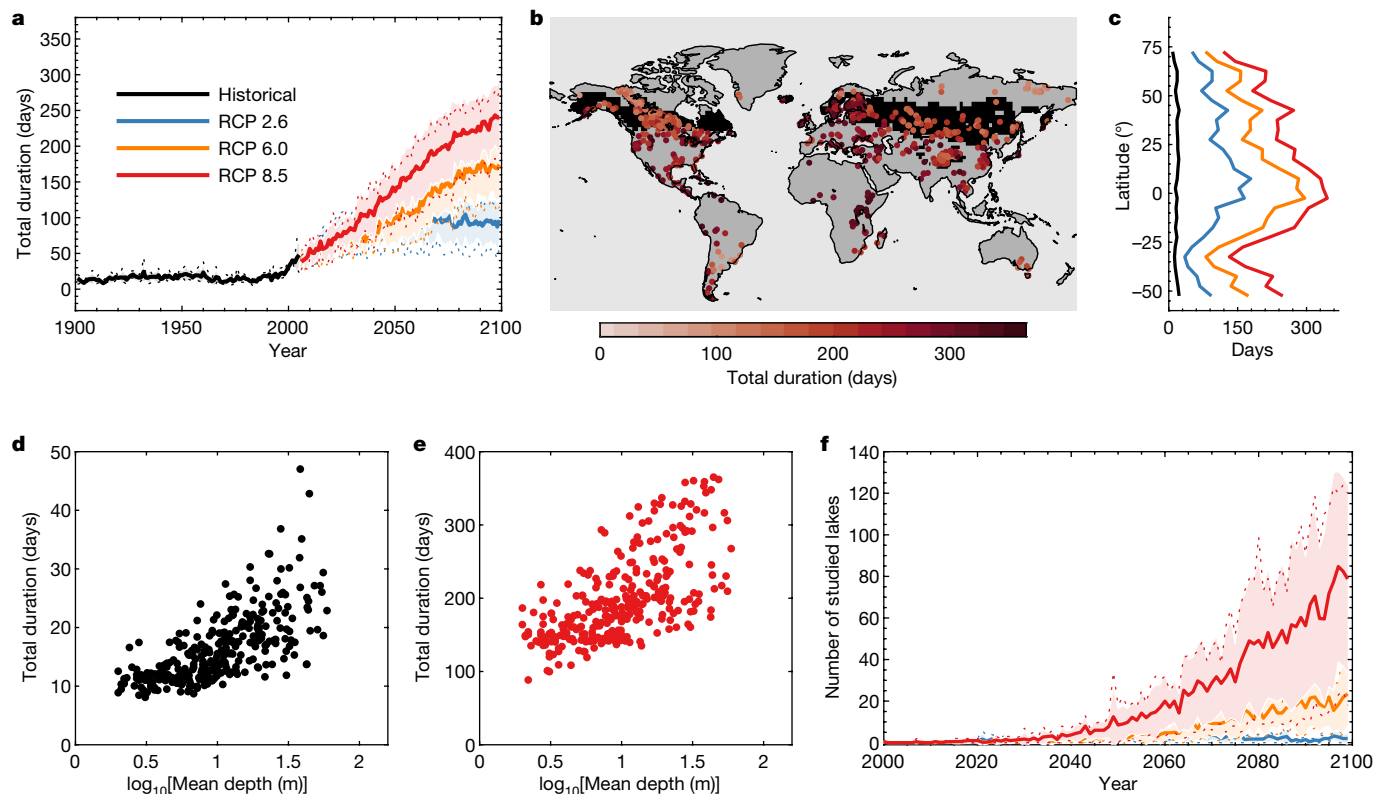


**Fig. 4 | Total heatwave duration and the emergence of a permanent heatwave state in lakes globally. a, b,** Temporal and spatial patterns in the total annual duration of lake heatwaves per year under twentieth and twenty-first century climate change. Time series are shown from 1901 to 2099 under historic and future climate forcing (RCP 2.6, RCP 6.0 and RCP 8.5). The thick lines demonstrate the mean across all studied lakes, the shaded regions represent the standard deviation, and the dashed lines represent the range across the lake-climate model ensembles. **b,** The total duration of simulated lake heatwaves per year by the end of the twenty-first century (averaged for all years from 2070 to 2099) under RCP 8.5. **c,** The latitudinal averages (5° bins) of

the lake heatwave duration under historical (1970–1999) and future (2070–2099) forcing. **d, e,** The relationship between heatwave duration and average lake depth ( $\log_{10}$ ), under historic (black) and future (red; RCP 8.5) climate change for lakes situated in the Northern Cool thermal region (shown as black regions in panel **b**; relationships for other thermal regions are shown in Extended Data Figs. 7, 8). **f,** The number of studied lakes worldwide that will experience a permanent lake heatwave state under RCP 2.6, RCP 6.0 and RCP 8.5. All results are based on the average simulations from the lake model driven by the four climate models.

there will be a substantial departure from the ‘normal’ lake heatwave conditions that have shaped lake ecosystems in the past towards a new norm. This also suggests that the baseline period to maintain a 90th percentile definition into the future should also be changed, for studies aiming to understand the true extremes for any specific time period. The lake heatwave metric used here uses historic conditions as a baseline. As lake temperatures increase during the twenty-first century, heatwaves in the past sense will no longer be extreme and will become the new normal. If understanding extremes for a specific time period is intended, then temperatures should be compared to climatological conditions over a sliding 30-year window that removes the long-term warming signal. When we calculated heatwaves in this way our simulations show that the surface temperature of the studied lakes will warm considerably during the twenty-first century (Extended Data Fig. 9c). We test the influence of mean twenty-first century surface temperature change on lake heatwaves by repeating our analysis after detrending the lake surface temperature anomalies; that is, after removing the long-term warming signal<sup>15</sup>. Although these metrics no longer strictly capture heatwaves, at least according to the definitions of refs.<sup>12–14,16,17,19</sup>, they are still useful in identifying extremes for any specific time period and for investigating the primary drivers. The detrended surface temperature anomalies still demonstrate an increase in ‘heatwave’ intensity and duration during the twenty-first century (under RCP 8.5). However, these changes are much reduced compared to those calculated when the long-term warming signal is included,

particularly in terms of intensity, which is influenced considerably by the mean warming rate<sup>26</sup>.

The choice of baseline and whether or not to detrend a time series before calculating lake heatwaves<sup>15</sup> depends on the application. A fixed baseline, as we have used here, is appropriate for understanding impacts on species that adapt slowly (at evolutionary timescales), for example, to identify how lake heatwaves may affect local species/ecosystems in the future. However, if a species can adapt over decadal timescales to changing temperatures, then a sliding baseline<sup>15</sup> might be more appropriate, although there would presumably be limits to the extent of possible adaptation. Given that micro-evolutionary rates for a given species are unlikely to change rapidly enough to account for general rates of warming over the twenty-first century, the ability of a species to survive, or the effects on its fitness through competition or interactions with other trophic levels, will depend on the tolerance and effects of the increased temperature. Thus, although many aspects of a species’ responses to shifting thermal regimes remain unclear, using a shifting baseline or a detrended time series might not be effective for determining the potential ecological effects that lake heatwaves may have in the future.

We expect that the increases in the intensity and duration of lake heatwaves that we have described here will emerge as agents of disturbance to lake ecosystems in the near future, as has already occurred on land during atmospheric heatwaves, with reported mass mortality of birds and mammals<sup>27,28</sup> and substantial effects on human health<sup>29</sup>. Moreover,

although atmospheric heatwaves in terrestrial environments can dissipate rapidly, lake heatwaves may dissipate at a much lower rate as a result of the higher thermal capacity of water than air, indirect effects of lake heatwaves on water level (caused by increased evaporation<sup>24</sup>) and on changing stratification and mixing patterns<sup>7</sup>, thus intensifying the ecological response. Aquatic organisms in regions close to their critical thermal maximum will be especially affected by lake heatwaves<sup>6</sup>, leading to possibly extreme population loss, as has been documented in the marine environment<sup>17</sup>. The effects of heatwaves on freshwater species might be mitigated by exploiting the temporal and spatial temperature variation within a lake, including phenological change<sup>30</sup> and a potential thermal refuge at depth<sup>31</sup>. However, phenological change can lead to food-web desynchronization<sup>32</sup> and the increased number of heatwave days that we forecast may limit a seasonal escape from thermal extremes; we note that a potential refuge in deeper and cooler water has not prevented past mortality events caused by thermal extremes<sup>6</sup>. In addition, dispersal to cooler sites at higher elevation, or higher latitude<sup>33,34</sup>, will be constrained by the fragmented nature of lakes in the landscape, exacerbated by the worldwide increase in the number of dams<sup>35</sup>. Where local extinctions and range contractions in lakes involve ‘keystone species’, ecosystem effects could be particularly severe, via habitat loss and alterations to food-web dynamics and species interactions. A departure from historical lake thermal conditions, in combination with increased anthropogenic dispersal, may allow non-native species from warmer regions to become established and thrive<sup>36</sup>, further disrupting freshwater food webs. These complex interactions are hard to forecast, but the extreme heatwave in the summer of 2003 in central Europe illustrated the range of effects that might be expected, including increased thermal stability and hypolimnetic oxygen depletion<sup>37</sup>, production of cyanobacterial blooms<sup>38</sup> and a regime shift from pelagic to benthic productivity<sup>39</sup>.

There is increasing appreciation of the link between climate change and more frequent, more numerous extreme events (including heatwaves but also storms<sup>40,41</sup> and droughts<sup>42</sup>) and concern over their ecological effects on freshwater. These sudden, short-term ‘pulse events’<sup>43</sup> are likely to amplify any negative consequences of long-term ‘ramp’ disturbances<sup>43</sup> such as warming water. Our projections of future increases of heatwave duration and intensity for lakes may be conservative, because climate models tend to underestimate the influence of climatic extremes on various ecosystems<sup>44</sup>. Nonetheless, our analysis of changes to the physical environment of lakes points towards emerging challenges for lake biodiversity and the benefits lakes provide to human populations.

## Online content

Any methods, additional references, Nature Research reporting summaries, source data, extended data, supplementary information, acknowledgements, peer review information; details of author contributions and competing interests; and statements of data and code availability are available at <https://doi.org/10.1038/s41586-020-03119-1>.

- O'Reilly, C. et al. Rapid and highly variable warming of lake surface waters around the globe. *Geophys. Res. Lett.* **42**, 10773–10781 (2015).
- Sharma, S., Jackson, D. A., Minns, C. K. & Shuter, B. J. Will northern fish populations be in hot water because of climate change? *Glob. Change Biol.* **13**, 2052–2064 (2007).
- Farmer, T. M., Marschall, E. A., Dabrowski, K. & Ludsin, S. A. Short winters threaten temperate fish populations. *Nat. Commun.* **6**, 7724 (2015).
- Hansen, G. J., Read, J. S., Hansen, J. F. & Winslow, L. A. Projected shifts in fish species dominance in Wisconsin lakes under climate change. *Glob. Change Biol.* **23**, 1463–1476 (2017).
- Jonsson, T. & Setzer, M. A freshwater predator hit twice by the effects of warming across trophic levels. *Nat. Commun.* **6**, 5992 (2015).
- Till, A. et al. Fish die-offs are concurrent with thermal extremes in north temperate lakes. *Nat. Clim. Change* **9**, 637–641 (2019).
- Woolway, R. I. & Merchant, C. J. Worldwide alteration of lake mixing regimes in response to climate change. *Nat. Geosci.* **12**, 271–276 (2019).

- Maberly, S. C. et al. Global lake thermal regions shift under climate change. *Nat. Commun.* **11**, 1232 (2020).
- Abell, R. et al. Freshwater ecoregions of the world: a new map of biogeographic units for freshwater biodiversity conservation. *Bioscience* **58**, 403–414 (2008).
- Fischer, E. M. & Schär, C. Consistent geographical patterns of changes in high-impact European heatwaves. *Nat. Geosci.* **3**, 398–403 (2010).
- Seneviratne, S. I. et al. in *Managing the Risks of Extreme Events and Disasters to Advance Climate Change Adaptation* (eds Field, C. B. et al.) 109–230 (Cambridge Univ. Press, 2012).
- Frölicher, T. L., Fischer, E. M. & Gruber, N. Marine heatwaves under global warming. *Nature* **560**, 360–364 (2018).
- Oliver, E. C. J. et al. Longer and more frequent marine heatwaves over the past century. *Nat. Commun.* **9**, 1324 (2018).
- Oliver, E. C. J. et al. Projected marine heatwaves in the 21st century and the potential for ecological impact. *Front. Mar. Sci.* **6**, 734 (2019).
- Jacox, M. G., Alexander, M. A., Bograd, S. J. & Scott, J. D. Thermal displacement by marine heatwaves. *Nature* **584**, 82–86 (2020).
- Holbrook, N. J. et al. A global assessment of marine heatwaves and their drivers. *Nat. Commun.* **10**, 2624 (2019).
- Smale, D. A. et al. Marine heatwaves threaten global biodiversity and the provision of ecosystem services. *Nat. Clim. Change* **9**, 306–312 (2019).
- Rasconi, S., Winter, K. & Kainz, M. J. Temperature increase and fluctuation induce phytoplankton biodiversity loss. Evidence from a multi-seasonal mesocosm experiment. *Ecol. Evol.* **7**, 2936–2946 (2017).
- Hobday, A. J. et al. A hierarchical approach to defining marine heatwaves. *Prog. Oceanogr.* **141**, 227–238 (2016).
- Hobday, A. J. et al. Categorizing and naming marine heatwaves. *Oceanography* **31**, 162–173 (2018).
- Messenger, M. L., Lehner, B., Grill, G., Nedeva, I. & Schmitt, O. Estimating the volume and age of water stored in global lakes using a geo-statistical approach. *Nat. Commun.* **7**, 13603 (2016).
- Woolway, R. I. & Merchant, C. J. Amplified surface temperature response of cold, deep lakes to inter-annual air temperature variability. *Sci. Rep.* **7**, 4130 (2017).
- Toffolon, M. et al. Prediction of surface temperature in lakes with different morphology using air temperature. *Limnol. Oceanogr.* **59**, 2185–2202 (2014).
- Wang, W. et al. Global lake evaporation accelerated by changes in surface energy allocation in a warmer climate. *Nat. Geosci.* **11**, 410–414 (2018).
- Weyhenmeyer, G. A., Westöo, A. K. & Willén, E. in *European Large Lakes: Ecosystem Changes And Their Ecological And Socioeconomic Impacts* (eds Nöges T. et al.) 111–118 (Springer, 2007).
- Oliver, E. C. J. Mean warming not variability drives marine heatwave trends. *Clim. Dyn.* **53**, 1653–1659 (2019).
- Welbergen, J. A., Klose, S. M., Markus, N. & Eby, P. Climate change and the effects of temperature extremes on Australian flying-foxes. *Proc. R. Soc. Lond. B* **275**, 419–425 (2008).
- Saunders, D. A., Mawson, P. & Dawson, R. The impact of two extreme weather events and other causes of death on Carnaby's Black Cockatoo: a promise of things to come for a threatened species? *Pacif. Conserv. Biol.* **17**, 141–148 (2011).
- Mitchell, D. et al. Attributing human mortality during extreme heat waves to anthropogenic climate change. *Environ. Res. Lett.* **11**, 074006 (2016).
- Thackeray, S. J. et al. Phenological sensitivity to climate across taxa and trophic levels. *Nature* **535**, 241–245 (2016).
- Winslow, L. A. et al. Small lakes show muted climate change signal in deepwater temperatures. *Geophys. Res. Lett.* **42**, 355–361 (2015).
- Thackeray, S. J. et al. Food web de-synchronization in England's largest lake: an assessment based on multiple phenological metrics. *Glob. Change Biol.* **19**, 3568–3580 (2013).
- Comte, L. & Grenouillet, G. Do stream fish track climate change? Assessing distribution shifts in recent decades. *Ecography* **36**, 1236–1246 (2013).
- Woolway, R. I. & Maberly, S. C. Climate velocity in inland standing waters. *Nat. Clim. Change* **10**, 1124–1129 (2020).
- Zarfl, C. et al. A global boom in hydropower dam construction. *Aquat. Sci.* **77**, 161–170 (2015).
- Muhlfeld, C. C. et al. Invasive hybridization in a threatened species is accelerated by climate change. *Nat. Clim. Change* **4**, 620–624 (2014).
- Jankowski, T. et al. Consequences of the 2003 European heat wave for lake temperature profiles, thermal stability, and hypolimnetic oxygen depletion: implications for a warmer world. *Limnol. Oceanogr.* **51**, 815–819 (2006).
- Jöhnk, K. et al. Summer heatwaves promote blooms of harmful cyanobacteria. *Glob. Change Biol.* **14**, 495–512 (2008).
- Bertani, I., Primicerio, R. & Rossetti, G. Extreme climatic event triggers a lake regime shift that propagates across multiple trophic levels. *Ecosystems* **19**, 16–31 (2016).
- Stockwell, J. D. et al. Storm impacts on phytoplankton community dynamics in lakes. *Glob. Change Biol.* **26**, 2756–2784 (2020).
- Woolway, R. I. et al. Physical and chemical impacts of a major storm on a temperate lake: a taste of things to come? *Clim. Change* **151**, 333–347 (2018).
- Zhou, Y., Michalak, A. M., Beletsky, D., Rao, Y. R. & Richards, R. P. Record-breaking Lake Erie hypoxia during 2012 drought. *Environ. Sci. Technol.* **49**, 800–807 (2015).
- Lake, P. S. Disturbance, patchiness, and diversity in streams. *J. N. Am. Benthol. Soc.* **14**, 573–592 (2000).
- Schewe, J. et al. State-of-the-art global models underestimate impacts from climate extremes. *Nat. Commun.* **10**, 1005 (2019).

**Publisher's note** Springer Nature remains neutral with regard to jurisdictional claims in published maps and institutional affiliations.

© The Author(s), under exclusive licence to Springer Nature Limited 2021

## Methods

### Study sites

The lakes investigated in this study ( $n = 702$ ) were selected based on the availability of satellite-derived lake surface temperature observations worldwide, in addition to the availability of mean depth information for lakes globally. The lakes studied vary in their geographic and morphological characteristics (Extended Data Fig. 2a–c).

### Observed lake surface temperatures

In this study, we use lake surface temperatures generated by ref. <sup>45</sup> using data from the Along Track Scanning Radiometer (ATSR) series of sensors including ATSR-2 (1995–2003) and the Advance ATSR (AATSR) (2002–2005). Lake surface temperature observations were retrieved following the methods of ref. <sup>46</sup> on image pixels filled with water according to both the inland water dataset of ref. <sup>47</sup> and a reflectance-based water detection scheme. The data (version 4.0) are available at daily resolution from the Global Observatory of Lake Responses to Environmental Change (GloboLakes; <https://catalogue.ceda.ac.uk/uuid/76a29c5b55204b66a40308fc2ba9cdb3>). Lake mean surface temperature time series were obtained by averaging across the surface area of each lake. Lake mean surface temperatures were used in this study to average across the intra-lake heterogeneity of surface water temperature responses to climate change<sup>48</sup> and to correspond to the lake mean model used (see below). For satellite-derived lake surface temperatures, the obtained value is sensitive to the skin temperature of the water, which is the temperature of a layer <0.1 mm thick from which thermal radiation is emitted by the lake. Thus, the satellite data are an estimate of this skin temperature, which may differ from the temperature as measured by a thermometer a few centimetres below the water–air interface. Typically, the temperature difference between skin and sub-skin lake surface temperature is of the order of 0.2 °C. However, the difference depends on meteorological conditions (for example, wind speed). Although the skin effect is variable, the satellite lake surface temperature is nonetheless tightly coupled to the lake surface temperature as measured conventionally. Satellite lake surface temperatures have been used to quantify worldwide aspects of lake thermal dynamics such as seasonal cycles<sup>8</sup>, onset of summer stratification<sup>48</sup>, lake mixing dynamics<sup>7</sup> and over-turning behaviour<sup>49</sup>. As an additional validation, we also compared the simulated lake surface temperatures with those available from the European Space Agency's (ESA) Climate Change Initiative (CCI) Lakes project (<http://cci.esa.int/lakes>), which provides daily observations of lake surface temperature at a grid resolution of 1/120° for 250 lakes worldwide, following the procedure used by ref. <sup>34</sup>.

### Simulated lake surface temperatures

The surface temperature (and ice cover) of lakes (notably the temperature of the upper well-mixed layer, the depth of which is defined according to the maximum vertical density difference) globally were simulated in this study via the Freshwater Lake model (FLake)<sup>50,51</sup>, which has been tested extensively in past studies. FLake is used widely both for research and as a component in numerical weather prediction<sup>52–55</sup>. FLake is particularly suitable for global lake modelling as it is based on the concept of self-similarity of the temperature–depth curve, which results in low computational cost. Moreover, it contains few lake-specific model parameters and does not require extensive calibration. The model has been shown to provide accurate representation of the evolving temperature cycle of lakes worldwide. The performance of FLake has been tested across a spectrum of lake contexts and validated simulations of lake thermal responses to climate change as well as extreme atmospheric events<sup>7,56</sup>. It has also been compared with other more sophisticated, but computationally expensive, models and these studies demonstrate that FLake can consistently accurately simulate lake surface water temperatures with comparable skill and good

agreement with observations<sup>57</sup>. In brief, FLake is based on a two-layer parametric representation of the time-evolving temperature profile and on the integral budgets of heat and kinetic energy. The integrated approach implemented in FLake allows a realistic representation of the major physics behind turbulent and diffusive heat exchange in lakes; it includes an ice module, and a module to describe the vertical temperature structure of the thermally active layer of bottom sediments, as well as its interaction with the water column above. FLake was developed to simulate the thermal dynamics of lakes shallower than approximately 60 m (see for example ref. <sup>54</sup>), and thus when selecting the studied lakes this depth limitation was considered. Therefore, the deepest lakes included in this study have an average depth of about 60 m. In this study we also set a lower limit of 2 m for the selected lakes, as FLake has been shown previously to produce a considerable bias in surface temperature during summer in very shallow systems. FLake was also developed to simulate the thermal dynamics of freshwater lakes. Thus, hyper-saline lakes were not included in this study. However, previous studies have demonstrated the ability of the model to simulate accurately the surface conditions of lakes along salinity gradients<sup>8,54,58–60</sup> and FLake is even used in numerical weather prediction models to simulate shallow coastal waters (for example, ECMWF's Integrated Forecasting System)<sup>54</sup>. Thus, while we caution against the use of FLake for simulating the thermal dynamics of brackish lakes, particularly without modifying the model source code<sup>61</sup>, we include some brackish lakes here given that validation data was available, and the model performed well when compared to observations of both surface temperature and the lake heatwave metrics investigated.

The meteorological variables required to drive FLake are air temperature at 2 m, wind speed at 10 m, surface solar and thermal radiation, atmospheric pressure, and specific humidity. These atmospheric drivers were downloaded for this study from four bias-corrected (to the EWEMBI reference dataset<sup>62,63</sup>) climate model projections from the Inter-Sectoral Impact Model Intercomparison Project phase 2b (ISIMIP2b), HadGEM2-ES, GFDL-ESM2M, IPSL-CM5A-LR, and MIROC5, for the historic and future periods under three climate change scenarios: RCP 2.6, RCP 6.0 and RCP 8.5. These data were available at a daily timestep and at a grid resolution of 0.5° × 0.5°. Time series data were extracted for the grid point situated closest to the centre of each studied lake, defined as the maximum distance to land<sup>47</sup>. As the bias-corrected climate projections were available at a daily timestep, the lake temperature simulations from FLake in this study were also generated at a daily resolution. However, an important consideration in lake modelling is that the timestep chosen to run a model can influence the accuracy of the simulations owing to, for example, the importance of diurnal forcing and the description of within-lake turbulence. These features can only be resolved fully when using high (for example, sub-hourly) temporal resolution data, and some studies have shown improved lake model performance when using sub-daily (compared to daily) data over short time periods<sup>64</sup>. However, for long-term global lake-climate projections, the temporal resolution of the input data (hourly versus daily) has been shown to have relatively minimal influence, at least in one case study site<sup>65</sup>. In this study, we investigate the influence of model timestep in simulating lake heatwaves by comparing, for three case study sites (Extended Data Fig. 10), modelled lake heatwave intensity and duration by the end of the twenty-first century. Specifically, we compare the heatwave metrics from the original daily FLake simulations to those driven by the climate model projections which we temporally disaggregated, following the methods of ref. <sup>66</sup>, to a 3-h timestep. The results demonstrate only minor differences between the model simulations across the case study sites thus suggesting, for this study, that daily data are sufficient and can simulate lake heatwave responses to climate change.

Lake specific parameters must be set to simulate individual lakes optimally in FLake. These parameters comprise fetch (in metres), which we fix in this study to the square root of lake surface area, lake depth,

lake ice albedo and the light attenuation coefficient ( $K_d$ , in  $m^{-1}$ ). The prognostic variables needed to initialize FLake simulations include (i) mixed layer temperature, (ii) mixed layer depth, (iii) bottom temperature, (iv) temperature at the ice (if present) upper surface and (v) ice thickness (if present). To initialize the model runs from physically reasonable fields, we initialize runs from a perpetual-year solution for the lake state. To find this solution for the initialization state, the model parameters are set as follows: mean depth was extracted from the Hydrolakes database<sup>21</sup>, and lake ice albedo was set to 0.6 (ref. <sup>51</sup>). The Hydrolakes data (specifically those for lake depth) have been extensively validated by ref. <sup>21</sup>, including detailed validations using approximately 12,000 records of observations. The atmospheric forcing data to derive the initialization conditions are from the ERA5 reanalysis product<sup>67</sup>, available at a latitude and longitude resolution of  $0.25^\circ$ . To optimize FLake simulations for each lake, and to approximate  $K_d$ , we use the model-tuning algorithm of ref. <sup>68</sup>. Prior to running the model-tuning algorithm we first approximate  $K_d$  for each study site according to  $K_d = 5.681 \times \text{depth}^{-0.795}$  ( $R_{\text{adj}}^2 = 0.51$ , degrees of freedom = 1,256). This relationship was derived from Secchi depth ( $Z_{\text{secchi}}$ ) measurements in 1,183 lakes in the US-EPA's National Lakes Assessment<sup>69</sup> and 75 lakes from the World Lake Database (<http://wldb.ilec.or.jp/>). Secchi depth was converted to extinction coefficients with the standard relationship of  $K_d = 1.7/Z_{\text{secchi}}$  (ref. <sup>70</sup>). These initial  $K_d$  values were then used as an initialization value within the tuning algorithm. The optimization routine estimates  $K_d$  to closely reproduce the observed seasonal and inter-annual surface temperature dynamics (1995 to 1999), specifically by minimizing the mean square differences between the model and satellite-derived surface water temperatures described above, in simulations initialized from the perpetual-year solution. The lake-specific parameters for the model are thus set without reference to any of the climate model forcing fields used for the historical-period simulation and future projections. A 51-year spin-up period (1850–1900) for each lake was also used in this study. As there is no water balance equation in FLake, lake depth and surface area are constant in time. Although this is common in global lake modelling<sup>24,54</sup>, the dynamic representation of lakes within the Earth system is a priority for future research.

In this study, the 'snow block' of FLake was not used, so the simulated ice cover dynamics of some lakes might be over- or underestimated, owing to the lack of snow on ice. Specifically, greater snow cover can delay or hasten ice breakup, respectively, through higher albedo (positive feedback) or greater insulation (negative or positive feedback, depending on the season). However, the model has been used previously to estimate successfully the ice cover dynamics of lakes globally, and been extensively validated with data from, for example, the National Snow and Ice Data Center and from the Interactive Multisensor Snow and Ice Mapping System<sup>54,71</sup>.

### Lake heatwave definitions

Lake heatwave intensity and duration were calculated from daily lake surface temperature time series following the methods described by ref. <sup>19</sup> for defining heatwaves in marine environments. Specifically, the R package 'heatwaveR'<sup>72</sup> was used for these calculations. Lake heatwaves were identified to occur when daily lake surface temperatures, specifically the average temperature of the upper mixed layer (which has a more direct influence on the ecosystem compared to, for example, the upper 1 m), were above a local and seasonally varying 90th percentile threshold (Extended Data Fig. 1). These anomalies were calculated for each calendar day using the daily temperatures within an 11-day window centred on the date across all years within the climatological period (1970–1999) and smoothed by applying a 31-day moving average<sup>19</sup>. An 11-day window and a 31-day moving average were selected to ensure a sufficient sample size for percentile estimation as well as a smooth climatological mean<sup>13,19</sup>. In addition, the 90th percentile threshold had to be exceeded for at least five consecutive days to be considered

a lake heatwave event, and two events with a break of less than three days were considered as a single event. Ideally, this definition should be relevant to ecological processes and thresholds (for example, based on evidence of impact on specific species). However, for this global-scale analysis, we follow the recommendations of ref. <sup>19</sup> of a five-day exceedance condition. Future studies should investigate thermal extreme indicators based on, for example, thermal tolerance limits of individual species. A statistical percentile-based threshold is useful because lake ecosystems are, to some degree, adapted to their own climate and so a statistical extreme is likely also to be an extreme in ecosystem functioning. In addition, the use of a percentile-based and seasonally varying threshold allows quantification of lake heatwaves across locations that differ in variability and mean conditions (Extended Data Fig. 2d–g) and to identify anomalously warm events at any time of the year, rather than events only during the warmest month. An absolute threshold would only be relevant in terms of impacts in some regions and seasons but not others (for example, due to species acclimation).

In this study we investigated lake heatwave metrics related to their duration and intensity. We also use an intensity-based lake heatwave category to define the strength of lake heatwaves. Each lake heatwave event was classified as being Moderate, Strong, Severe or Extreme. These categories are defined by the maximum intensity of the event scaled by the threshold temperature anomaly exceeding the climatological mean<sup>20</sup>. For example, Moderate events are those with lake temperature anomalies that exceed the identified threshold but are less than 2 times that threshold value; Strong, Severe and Extreme events are then identified according to anomalies that exceed 2, 3 and 4 times that threshold value, respectively (Extended Data Fig. 1). The season(s) during which lake heatwaves occur are also investigated in this study. June is used as the start of boreal summer and December as the start of austral summer. When calculating the time series of annual average intensity and average duration of lake heatwave events, we separated heatwaves into two events if they lasted beyond 31 December. Thus, the maximum duration of a lake heatwave in this study is 366 days.

In this study, following ref. <sup>15</sup>, we also calculate lake heatwaves based on detrended lake surface temperature anomalies (Extended Data Fig. 9d–f) in order to illustrate the influence on lake heatwaves of mean lake temperature change versus changes in variance, both of which are considered important for the future occurrence of heatwave events. However, we do stress that by detrending the lake surface temperature anomalies, one is no longer explicitly analysing lake heatwaves, at least according to the definitions commonly used for marine heatwaves<sup>12–14,16,17,19</sup>. To compare heatwaves across realms (for example, ocean versus lakes), a consistent methodology (to the extent possible) should be adopted.

### Validation of simulated lake heatwaves

Owing to the dearth of long-term in situ high-resolution data available for lakes<sup>73</sup>, the simulated intensity and duration of lake heatwaves could not be validated with in situ observations. However, the ability of the model to simulate lake heatwave events can be evaluated by comparing the simulations with those identified from the satellite observations. An issue when using satellite observations to identify lake heatwaves is that these data often contain gaps due to, for example, the presence of clouds, which will undoubtedly influence the identification of lake heatwaves. Some lakes do contain sufficient data to identify lake heatwaves at certain times of the year (for example, July–September), and thus to compare with the simulated heatwaves in some years. Specifically, in lakes with less than three consecutive days of missing data in a given time period, the temporal threshold used for determining whether a heatwave is considered a single event or multiple shorter events, we can estimate lake heatwaves from the satellite data. In our dataset, 190 globally distributed lakes have sufficient data for such



comparisons (Extended Data Fig. 3). For these lakes, we compare the observed and simulated average intensity and duration of lake heatwaves during July–September (or January–March; see below), the time of year in which most cloud-free satellite retrievals are available. By following the definitions of refs. <sup>1,74</sup>, we selected temperatures for a three-month period. For lakes situated in the Northern Hemisphere we used the period of 1 July to 30 September (JAS); whereas, in the Southern Hemisphere, we used 1 January to 31 March (JFM). Exceptions were latitudes less than 23.5°, for which the JAS metric was used south of the Equator and the JFM metric was used north of the Equator. This was done in order to avoid the cloudy wet season in the tropics and instead to collect data during the dry season, which allows for an increased number of cloud-free satellite observations<sup>74</sup>. We selected data from these months to define lake heatwaves. For this model validation, the climatological mean was calculated over the satellite period (1995–2005). To compare with the simulated lake heatwaves, we calculated the heatwave metrics from the average lake-climate model ensembles from 2000 to 2005 (that is, the years that were not used in the optimization of the model parameters). Good agreement is obtained between simulations and observations of lake heatwaves (Extended Data Fig. 3).

## Statistical methods

To investigate the influence of lake depth on the average intensity and duration of lake heatwaves, we first separated the studied lakes into the thermal regions in which they are located, following the definitions of ref. <sup>8</sup>. The thermal regions had been produced objectively using *b*-spline modelling and *K*-means clustering of satellite-derived seasonal lake surface water temperature data, for lakes globally over a period of 16 years. Within each lake thermal region, relationships between the response variables (heatwave duration and heatwave intensity) and the independent variable (mean depth; log<sub>10</sub> transformed) were assessed using generalized additive modelling with a cubic regression spline using cross-validation to optimize *k*, the number of knots in *R* (refs. <sup>75–77</sup>). The sequence of the analysis was guided by the protocol of ref. <sup>78</sup>. The residuals from each generalized additive model were first checked for any breach of assumptions. A variance structure was added to the models to account for unequal variance in residuals where appropriate. Where the estimated degrees of freedom equalled one, the generalized additive model was compared to a linear model and the optimum model was selected based on the Akaike information criterion. The *P* value presented is defined as the probability of getting a value of the test statistic that is at least as favourable to the alternative hypothesis as one actually observed if the null hypothesis is true<sup>75</sup>. For linear regression models we used a threshold for significance of *P* < 0.05. For generalized additive models we used a more conservative threshold of *P* < 0.001 (refs. <sup>75,78</sup>).

## In situ observations of lake heatwaves

In this study, we also calculate the intensity and duration of lake heatwaves in lakes where long-term in situ surface water temperature data are available. Specifically, by analysing published daily data from two European lakes<sup>79</sup>, Lake Vättern in Sweden (58.321° N, 14.467° E) and Wörthersee in Austria (46.628° N, 14.127° E), we investigate lake heatwave variability from 1960 to 2017. Although lake surface temperature measurements from these lakes are not directly comparable to those simulated in this study, given that they were either measured at a lake level gauging station (Wörthersee) or from a drinking water intake point (Vättern), they are useful to explore historical changes in lake heatwaves. Following the same definitions as above for defining simulated lake heatwaves, we demonstrate a considerable increase in heatwave duration in both lakes from 1960 to 2017. An increase in lake heatwave intensity is also calculated for Lake Vättern since 1960, but not in Wörthersee (Extended Data Fig. 1).

## Data availability

The lake model source code is available to download from <http://www.flake.igb-berlin.de/>. Climate model projections (ISIMIP2b; date accessed: August 01, 2020) are available at <https://www.isimip.org/protocol/#isimip2b>. Satellite-derived lake surface temperatures used in this study are available from <https://catalogue.ceda.ac.uk/uuid/76a29c5b55204b66a40308fc2ba9cddb3> (Globolakes; accessed 1 August 2020) and from <https://catalogue.ceda.ac.uk/uuid/3c324bb4ee394d0d876fe2e1db217378> (ESA CCI; accessed 1 August 2020). Data for the light extinction coefficient used in this study are from the United States Environmental Protection Agency National Lakes Assessment (<https://edg.epa.gov/metadata/catalog/search/resource/details.page?uuid=%7B668F7BE3-50D1-465C-A73D-B21625689159%7D>) and the World Lake Database (<http://wldb.ilec.or.jp/>). All lake heatwave simulations, as well as a table of lake-specific information, are available at <https://doi.org/10.5281/zenodo.4081165>.

## Code availability

The MATLAB code used to produce the figures in this paper are available at <https://doi.org/10.5281/zenodo.4081165>.

45. Carrea, L. & Merchant, C. J. *GloboLakes: Lake Surface Water Temperature (LSWT) version 4.0*, <https://catalogue.ceda.ac.uk/uuid/76a29c5b55204b66a40308fc2ba9cddb3> (Centre for Environmental Data Analysis, 2019).
46. MacCallum, S. N. & Merchant, C. J. Surface water temperature observations of large lakes by optimal estimation. *Can. J. Remote Sens.* **38**, 25–45 (2012).
47. Carrea, L., Embury, O. & Merchant, C. J. Datasets related to in-land water for limnology and remote sensing applications: distance-to-land, distance-to-water, water-body identifier and lake-centre co-ordinates. *Geosci. Data J.* **2**, 83–97 (2015).
48. Woolway, R. I. & Merchant, C. J. Intra-lake heterogeneity of lake thermal responses to climate change: a study of large Northern Hemisphere lakes. *J. Geophys. Res. Atmos.* **123**, 3087–3098 (2018).
49. Fichot, C. et al. Assessing change in the overturning behaviour of the Laurentian Great Lakes using remotely sensed lake surface water temperatures. *Remote Sens. Environ.* **235**, 111427 (2019).
50. Mironov, D. *Parameterization of Lakes in Numerical Weather Prediction: Part 1. Description of a Lake Model*. COSMO Technical Report No. 11, <http://www.cosmo-model.org> (Deutscher Wetterdienst, 2008).
51. Mironov, D. et al. Implementation of the lake parameterisation scheme FLake into the numerical weather prediction model COSMO. *Boreal Environ. Res.* **15**, 218–230 (2010).
52. Rooney, G. & Jones, I. D. Coupling the 1-D lake model FLake to the community land-surface model JULES. *Boreal Environ. Res.* **15**, 501–512 (2010).
53. Samuelsson, P., Kourzeneva, E. & Mironov, D. The impact of lakes on the European climate as simulated by a regional climate model. *Boreal Environ. Res.* **15**, 113–129 (2010).
54. Balsamo, G. et al. On the contribution of lakes in predicting near-surface temperature in a global weather forecasting model. *Tellus A* **64**, 15829 (2012).
55. Le Moigne, P., Colin, J. & Decharme, B. Impact of lake surface temperatures simulated by the FLake scheme in the CNRM-CM5 climate model. *Tellus A* **68**, 31274 (2016).
56. Woolway, R. I. et al. Impact of the 2018 European heatwave on lake surface water temperature. *Inland Waters* (2020).
57. Stepanenko, V. M. et al. First steps of a Lake Model Intercomparison Project: LakeMIP. *Boreal Environ. Res.* **15**, 191–202 (2010).
58. Thiery, W. et al. Understanding the performance of the FLake model over two African Great Lakes. *Geosci. Model Dev.* **7**, 317–337 (2014).
59. Thiery, W. V. et al. LakeMIP Kivu: evaluating the representation of a large, deep tropical lake by a set of one-dimensional lake models. *Tellus A* **66**, 21390 (2014).
60. Le Moigne, P. et al. Evaluation of the lake model FLake over a coastal lagoon during the THAUMEX field campaign. *Tellus A* **65**, 20951 (2013).
61. Su, D. et al. Numerical study on the response of the largest lake in China to climate change. *Hydrol. Earth Syst. Sci.* **23**, 2093–2109 (2019).
62. Frieler, K. et al. Assessing the impacts of 1.5°C global warming—simulation protocol of the Inter-Sectoral Impact Model Intercomparison Project (ISIMIP2b). *Geosci. Model Dev.* **10**, 4321–4345 (2017).
63. Lange, S. *Earth2Observe, WFDEI and ERA-Interim Data Merged and Bias-corrected for ISIMIP (EWEMBI) Version 1.1*. <https://doi.org/10.5880/pik.2019.004> (GFZ Data Services, 2019).
64. Bruce, L. C. A multi-lake comparative analysis of the General Lake Model (GLM): stress-testing across a global observatory network. *Environ. Model. Softw.* **102**, 274–291 (2018).
65. Ayala, A. I., Moras, S. & Pierson, D. C. Simulations of future changes in thermal structure of Lake Erken: proof of concept for ISIMIP2b lake sector local simulation strategy. *Hydrol. Earth Syst. Sci.* **24**, 3311–3330 (2020).
66. Shatwell, T. et al. Future projections of temperature and mixing regime of European temperate lakes. *Hydrol. Earth Syst. Sci.* **23**, 1533–1551 (2019).

67. Hersbach, H. et al. The ERA5 global reanalysis. *Quat. J. R. Meteorol. Soc.* **146**, 1999–2049 (2020).
68. Layden, A., MacCallum, S. N. & Merchant, C. J. Determining lake surface water temperatures worldwide using a tuned one-dimensional lake model (Flake, v1). *Geosci. Model Dev.* **9**, 2167–2189 (2016).
69. United States Environmental Protection Agency (USEPA). *National Lakes Assessment: A Collaborative Survey Of The Nation's Lakes*. <https://edg.epa.gov/metadata/catalog/search/resource/details.page?uuid=%7B668F7BE3-50D1-465C-A73D-B21625689159%7D> (USEPA, 2009).
70. Kirk, J. T. O. *Light and Photosynthesis in Aquatic Ecosystems* 3rd edn, 649 (Cambridge Univ. Press, 2011).
71. Helfrich, S. R., McNamara, D., Ramsay, B. H., Baldwin, T. & Kasheta, T. Enhancements to, and forthcoming developments in the Interactive Multisensor Snow and Ice Mapping System (IMS). *Hydrol. Process.* **21**, 1576–1586 (2007).
72. Schlegel, R. W. & Smit, A. J. *heatwaveR*: a central algorithm for the detection of heatwaves and cold-spells. *J. Open Source Softw.* **3**, 821 (2018).
73. Jennings, E. et al. The NETLAKE Metadatabase—a tool to support automatic monitoring on lakes in Europe and beyond. *Limnol. Oceanogr. Bull.* **26**, 95–100 (2017).
74. Schneider, P. & Hook, S. J. Space observations of inland water bodies show rapid surface warming since 1985. *Geophys. Res. Lett.* **37**, L22405 (2010).
75. Wood, S. N. *Generalized Additive Models: An Introduction With R* (CRC Press, 2017).
76. Pinheiro, J., Bates, D., DebRoy, S. & Sarkar, D. Linear and nonlinear mixed effects models. R package 'nlme', <https://CRAN.R-project.org/package=nlme> (2007).
77. R Core Team R: *A Language And Environment For Statistical Computing* <https://www.R-project.org/> (R Foundation for Statistical Computing, 2019).
78. Zuur, A. F., Ieno, E. N. & Walker, N. *Mixed Effect Models and Extensions in Ecology with R* (Springer, 2009).
79. Woolway, R. I. et al. Substantial increase in minimum lake surface temperatures under climate change. *Clim. Change* **155**, 81–94 (2019).

**Acknowledgements** R.I.W. received funding from the European Union's Horizon 2020 research and innovation programme under the Marie Skłodowska-Curie grant agreement number 791812. We thank the GloboLakes project (NE/J021717/1) and the Hydroscape project (NE/N00597X/1), funded by the Natural Environment Research Council in the United Kingdom. We also thank the Copernicus Climate Change Service Hydrology, funded by the European Union, and the European Space Agency Climate Change Initiative project for the satellite data. We also acknowledge the International Lake Environment Committee Foundation (ILEC, <http://www.ilec.or.jp/en/>), which maintains the World Lake Database (<http://wldb.ilec.or.jp/>). The computations and data handling were enabled by resources provided by the Swedish National Infrastructure for Computing (SNIC) at Uppmax, partially funded by the Swedish Research Council through grant agreement number 2016-07213. T.S. was partially supported by German Research Foundation grants DFG KI 853/13-1 and CDZ 1259.

**Author contributions** R.I.W. conceived the work, developed the concept of the study, performed the numerical modelling, completed the data analysis, and wrote the manuscript with input from S.C.M. All authors edited and revised the manuscript. T.S. performed the three-hour FLake simulations and led the light attenuation analysis, as used in the global simulations. E.J. performed the statistical analyses. M.G. and D.C.P. assisted with the large-scale computations and data handling.

**Competing interests** The authors declare no competing interests.

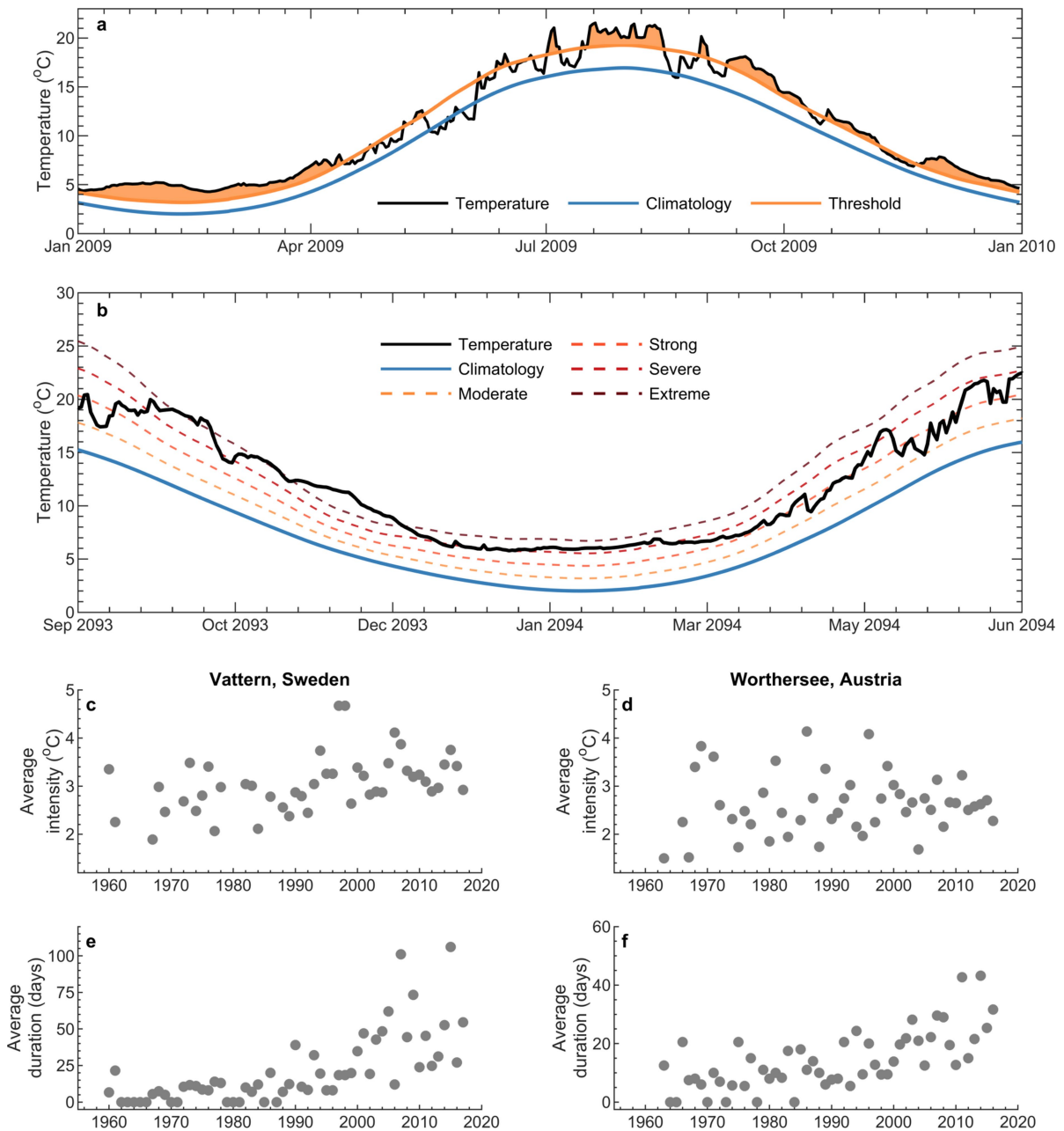
#### Additional information

**Supplementary information** is available for this paper at <https://doi.org/10.1038/s41586-020-03119-1>.

**Correspondence and requests for materials** should be addressed to R.I.W.

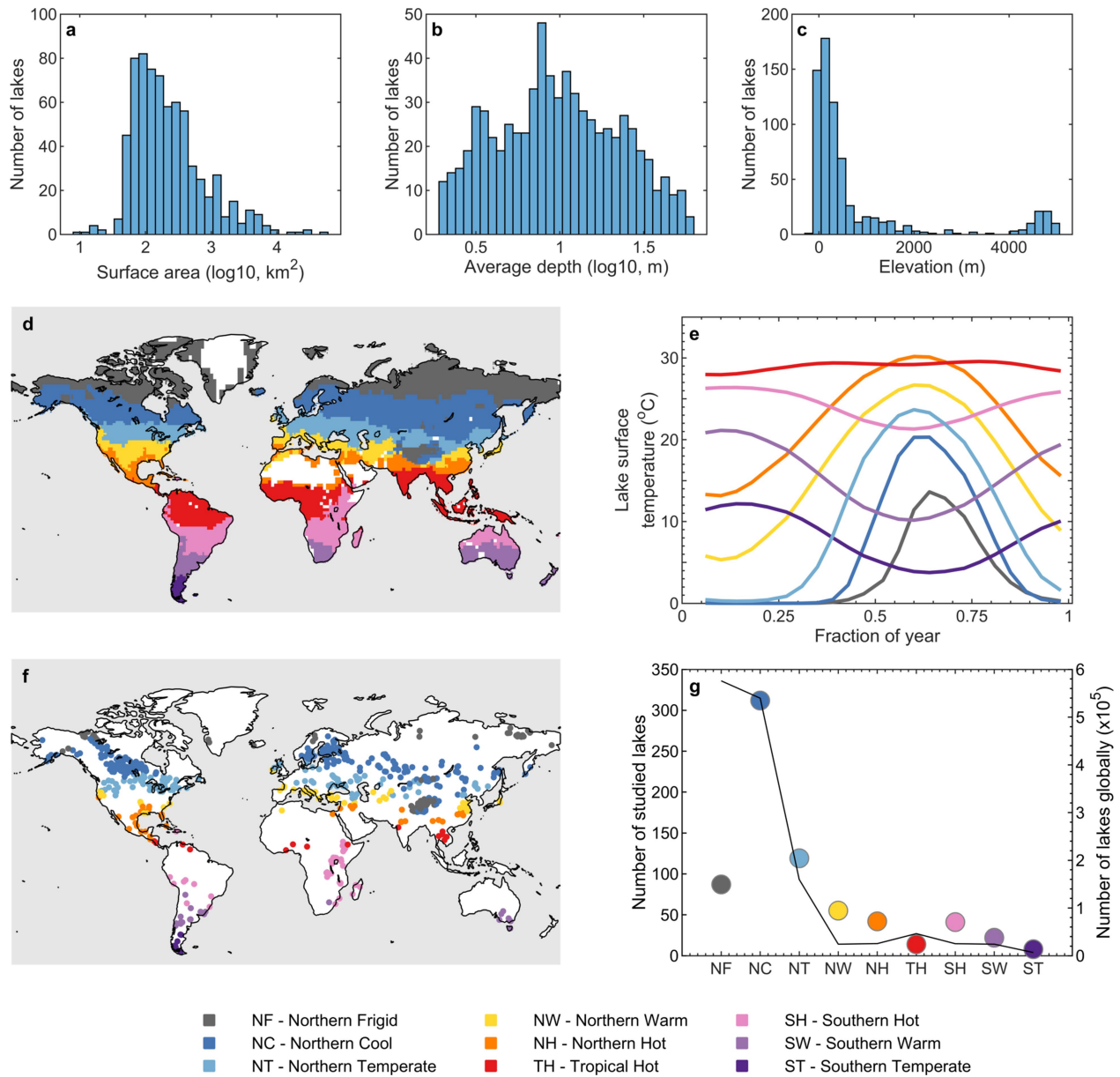
**Peer review information** *Nature* thanks Thomas Froelicher, Ekaterina Kurzeneva, Victor Stepanenko and the other, anonymous, reviewer(s) for their contribution to the peer review of this work. Peer reviewer reports are available.

**Reprints and permissions information** is available at <http://www.nature.com/reprints>.



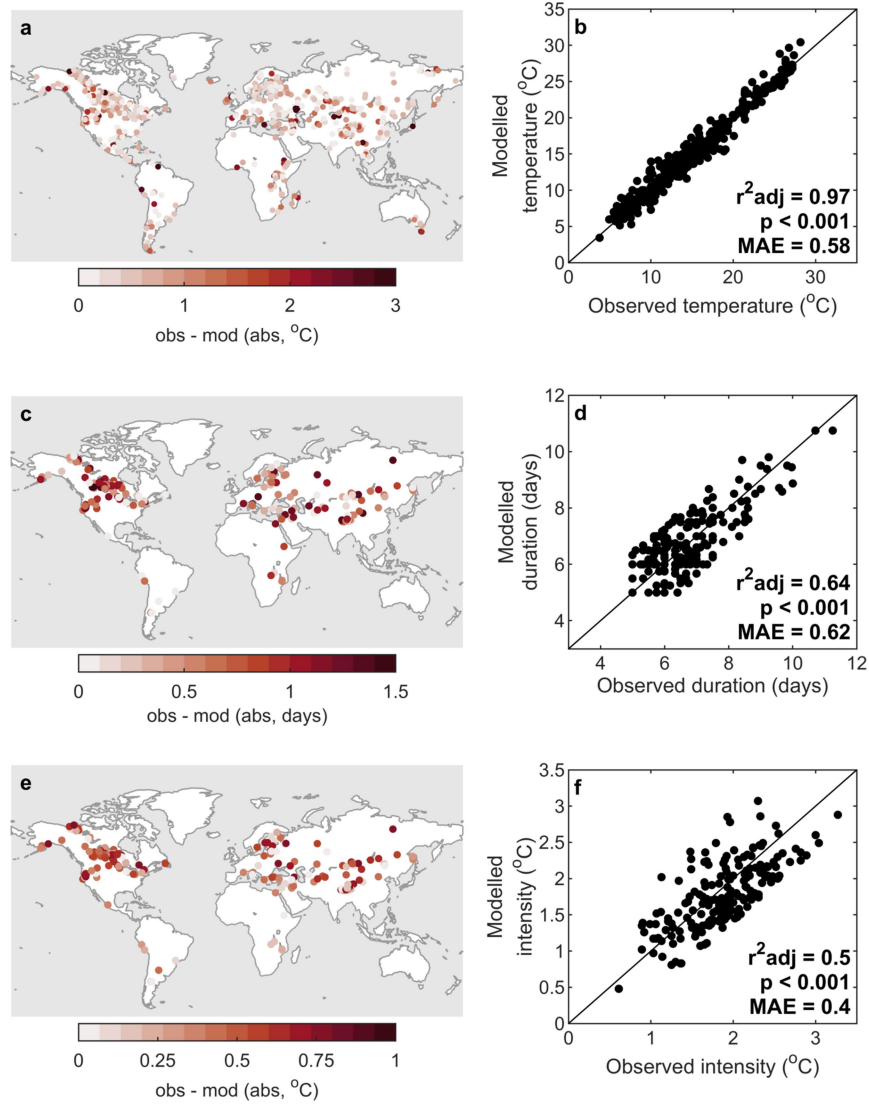
**Extended Data Fig. 1 | Definitions and examples of lake heatwaves.**  
**a, b**, Examples of the method used to define a lake heatwave event (light orange) from lake surface temperatures (black) (**a**) and the categorization scheme used for defining the severity of lake heatwaves (**b**). Lake heatwave categories are defined according to multiples of the 90th percentile differences (1, 2, 3 and 4 times the threshold) relative to a 30-year (1970–1999)

climatological mean (blue) and are described as Moderate (light orange), Strong (orange), Severe (red), or Extreme (dark red). Also shown are examples of historical lake heatwave intensity (**c, d**) and duration (**e, f**) in Lake Vättern (Sweden) (**c, e**) and Wörthersee (Austria) (**d, f**), where observational data are available from 1960 to 2017.



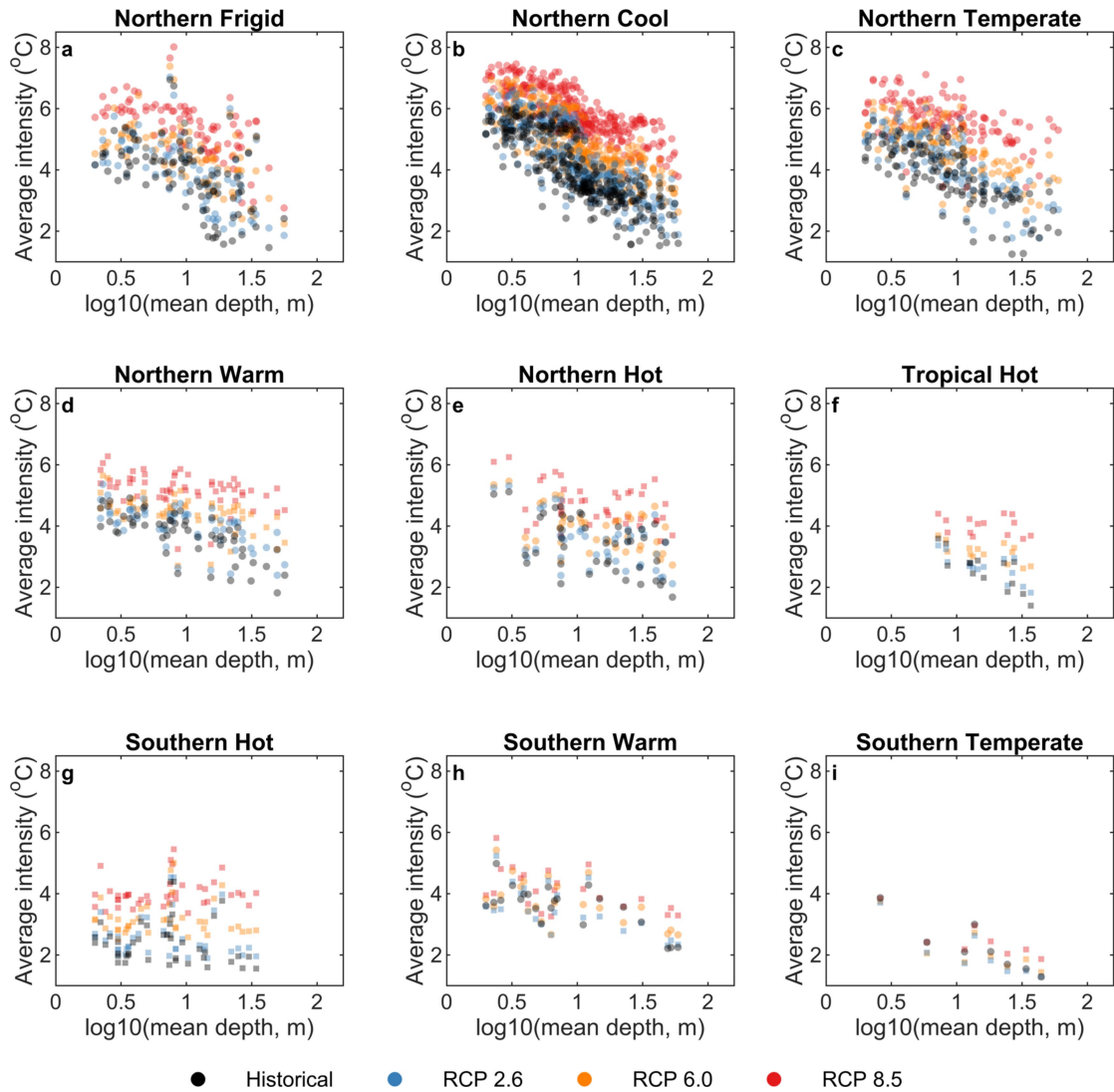
**Extended Data Fig. 2 | Specific characteristics of the studied lakes.** a-c, Histograms of  $\log_{10}[\text{surface area (km}^2\text{)}]$  (a),  $\log_{10}[\text{average depth (m)}]$  (b) and elevation (m) (c) of the lakes studied. d-g, We also show, for illustration, the global distribution of lake thermal regions (d), their climatological seasonal

cycle (e), a map of studied lakes categorized by thermal region (f), and the number of studied lakes (points) as well as the number of lakes globally (information from the Hydrolakes database<sup>21</sup>) situated within each lake thermal region (line) (g).



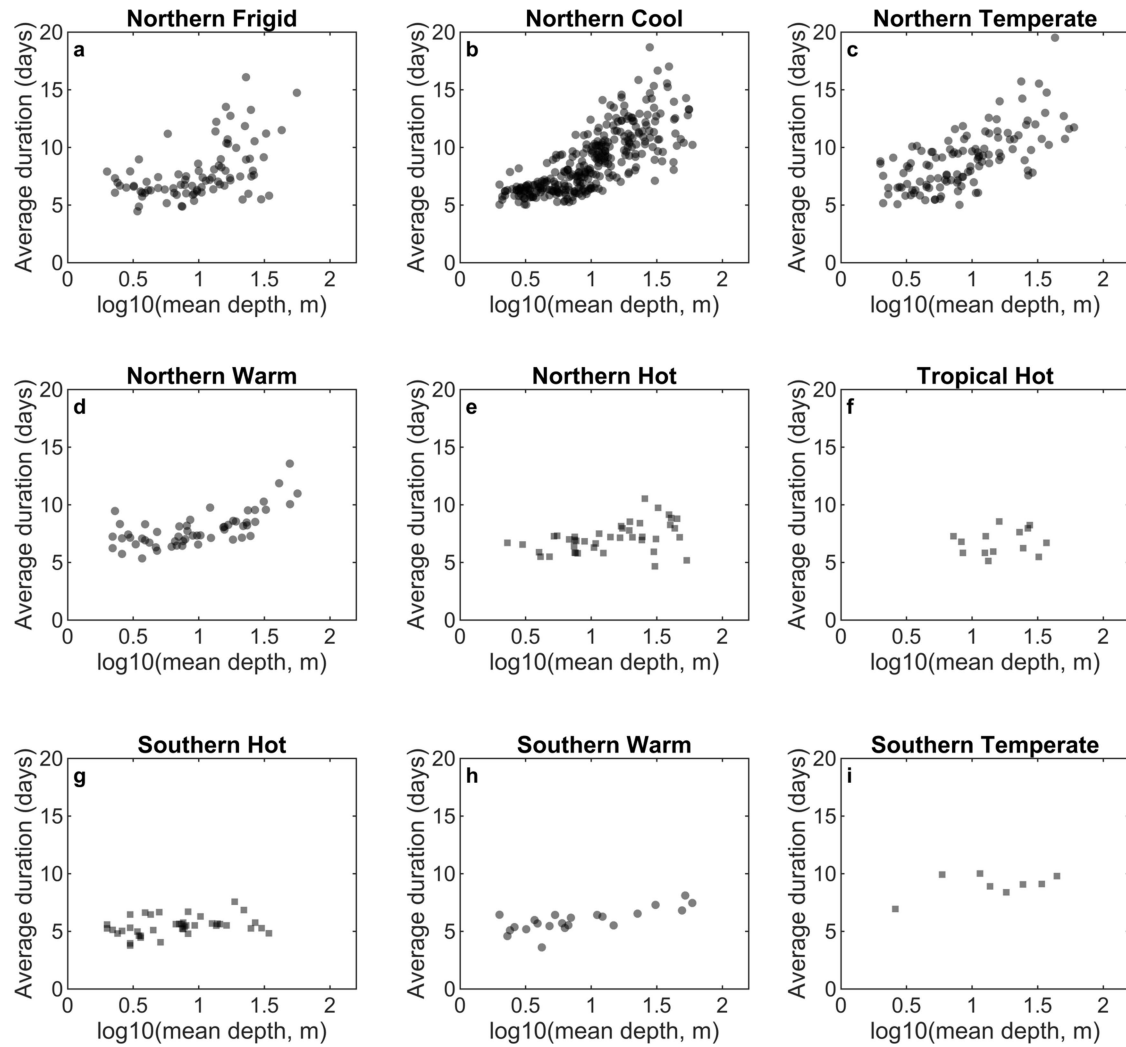
**Extended Data Fig. 3 | Validation of simulated lake temperatures and heatwave characteristics.** Comparison of modelled (mod) and satellite-observed (obs) (a, b) lake surface water temperatures for the studied lakes in which satellite data were available ( $R^2_{adj} = 0.97$ ,  $P < 0.001$ ); and lake heatwave duration ( $R^2_{adj} = 0.64$ ,  $P < 0.001$ ) (c, d) and intensity ( $R^2_{adj} = 0.5$ ,

$P < 0.001$ ) (e, f) for lakes with sufficient data to identify lake heatwaves from 2000 to 2005 (see Methods). Simulated results are based on the average simulations from the lake model driven by the four climate models. Abs, absolute; MAE, mean absolute error.



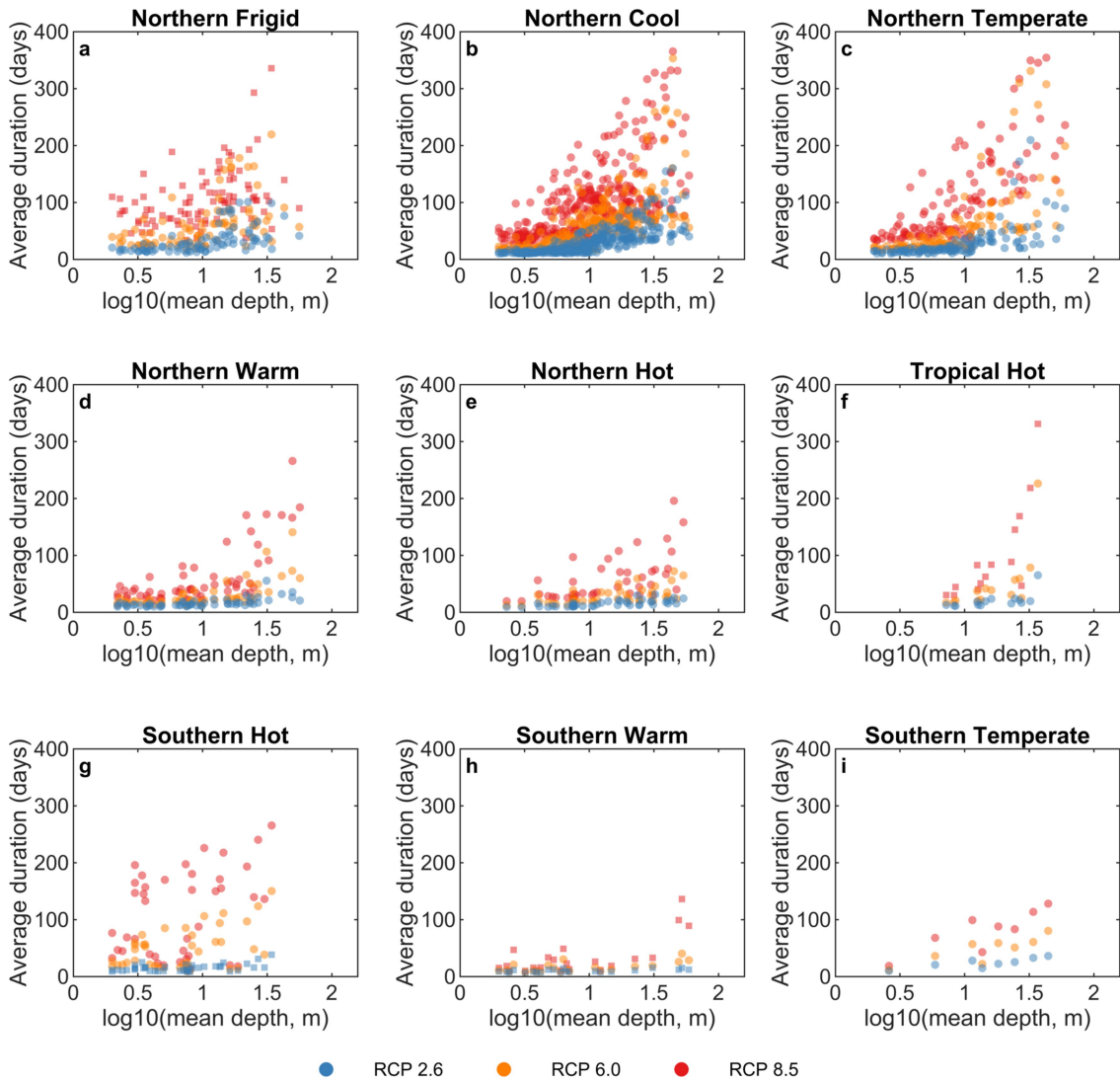
**Extended Data Fig. 4 | Relationship between average lake depth and average heatwave intensity.** For each lake thermal region, the relationship between  $\log_{10}$ [lake depth (m)] and the average intensity of lake heatwave events is shown for the historic period (averaged over all years from 1970 to 1999) and for the end of the twenty-first century (averaged over all years from 2070 to

2099) under RCP 2.6, RCP 6.0 and RCP 8.5. The relationships between lake depth and the heatwave metrics (square, not significant:  $P > 0.001$ ; circle, significant:  $P < 0.001$ ) were calculated with a generalized additive model (see Methods).



**Extended Data Fig. 5 | Relationship between average lake depth and average heatwave duration from 1970 to 1999.** For each lake thermal region, the relationship between  $\log_{10}[\text{lake depth (m)}]$  and the average duration of lake heatwave events is shown for the historic period (averaged over all years from

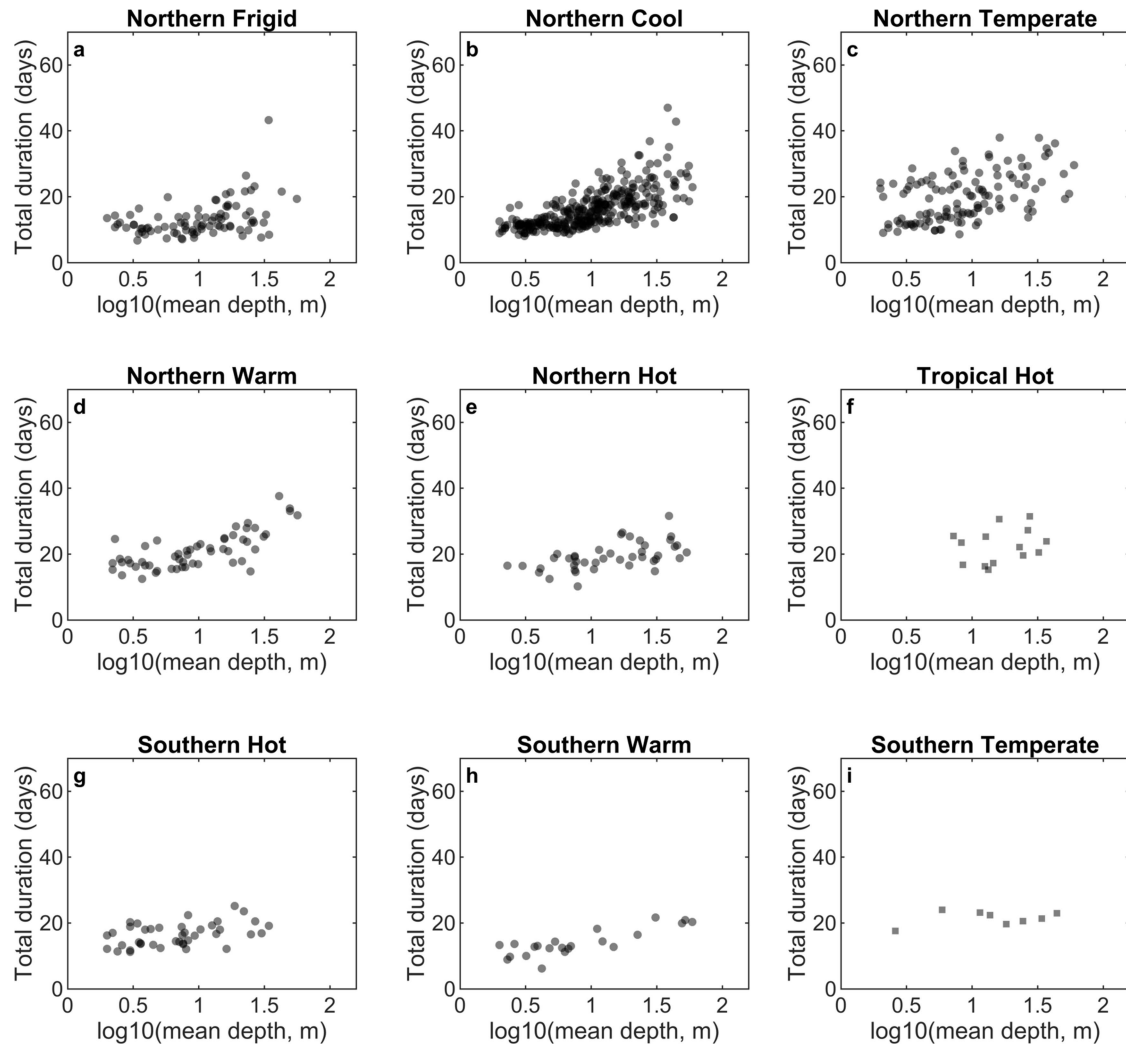
1970 to 1999). The relationships between lake depth and the heatwave metrics (square, not significant:  $P > 0.001$ ; circle, significant:  $P < 0.001$ ) were calculated with a generalized additive model (see Methods).



**Extended Data Fig. 6 | Relationship between average lake depth and average heatwave duration from 2070 to 2099.** For each lake thermal region, the relationship between  $\log_{10}$ [mean lake depth (m)] and the average duration of lake heatwave events is shown for the end of the twenty-first century

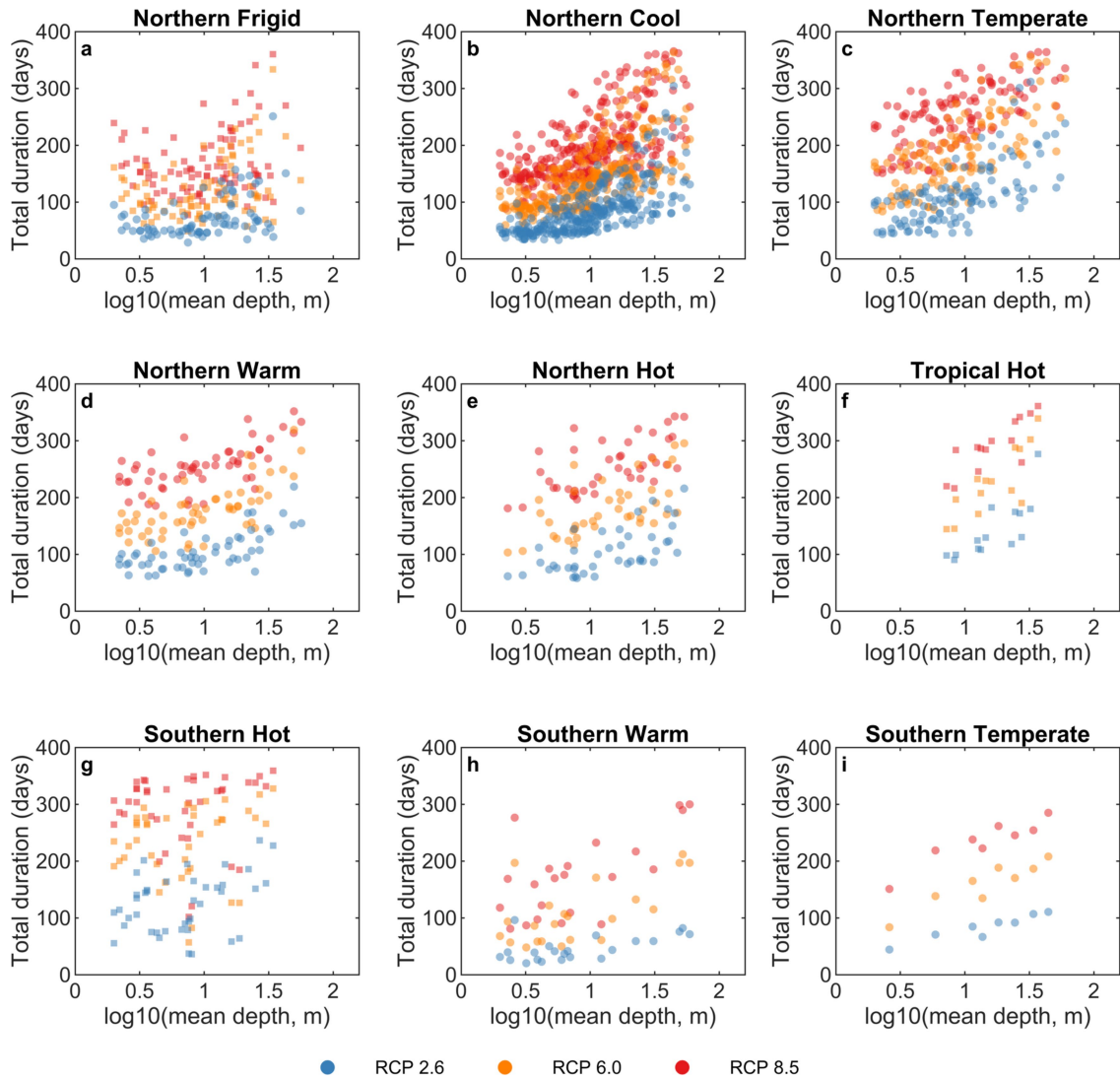
(averaged over all years from 2070 to 2099) under RCP 2.6, RCP 6.0 and RCP 8.5. The relationships between lake depth and the heatwave metrics (square, not significant:  $P > 0.001$ ; circle, significant:  $P < 0.001$ ) were calculated with a generalized additive model (see Methods).





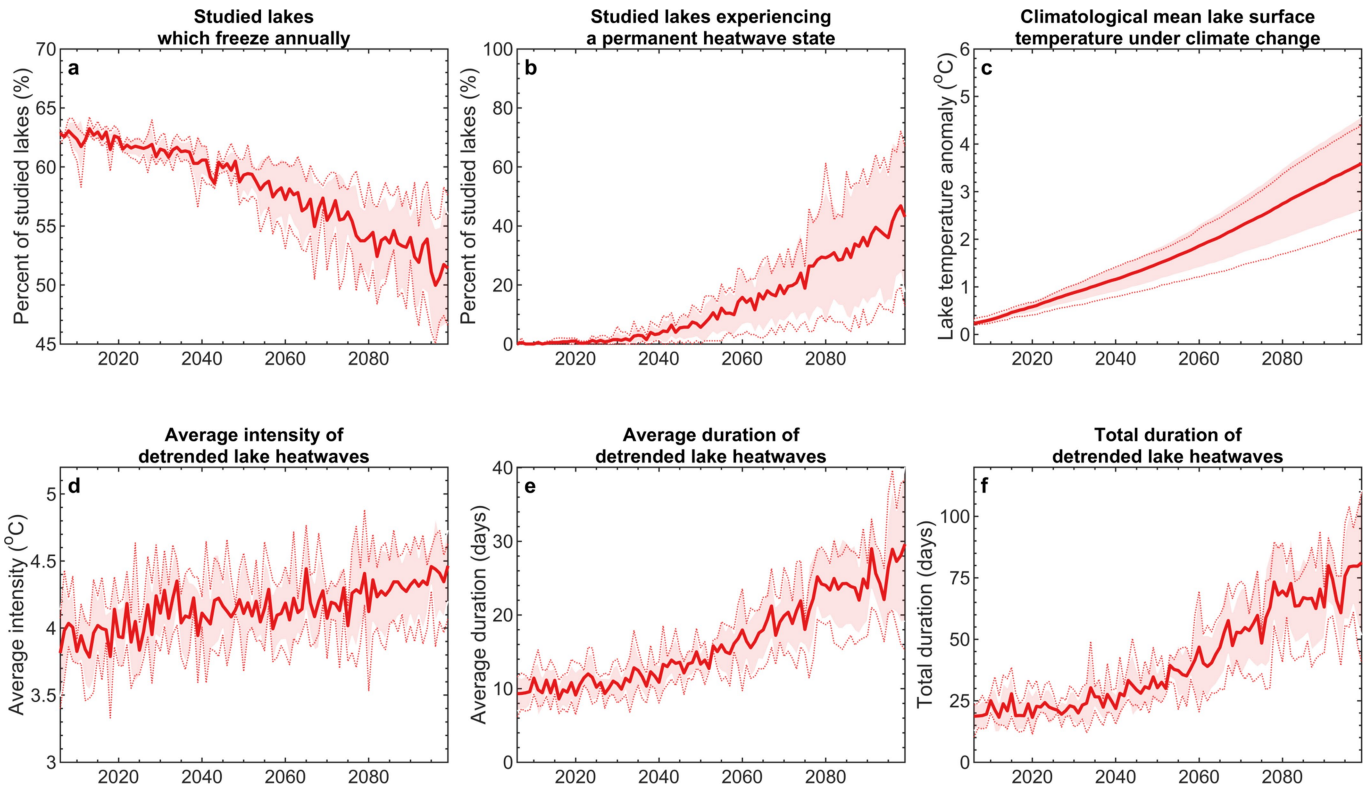
**Extended Data Fig. 7 | Relationship between average lake depth and total heatwave duration from 1970 to 1999.** For each lake thermal region, the relationship between  $\log_{10}$ [mean lake depth (m)] and the total duration of lake heatwave events per year is shown for the historic period (averaged over all

years from 1970 to 1999). The relationships between lake depth and the heatwave metrics (square, not significant:  $P > 0.001$ ; circle, significant:  $P < 0.001$ ) were calculated with a generalized additive model (see Methods).



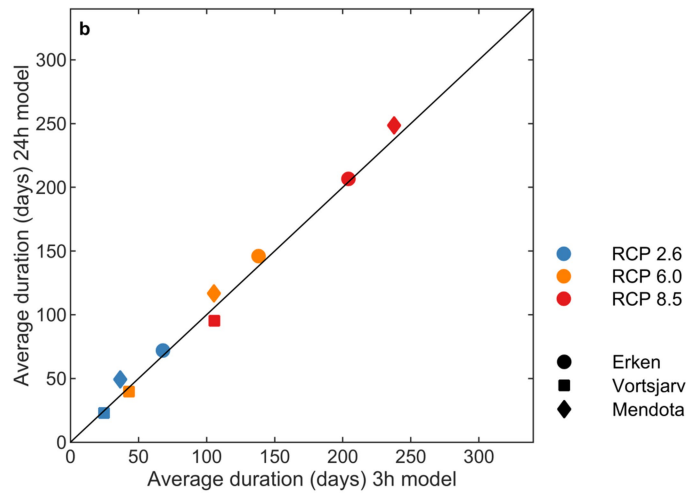
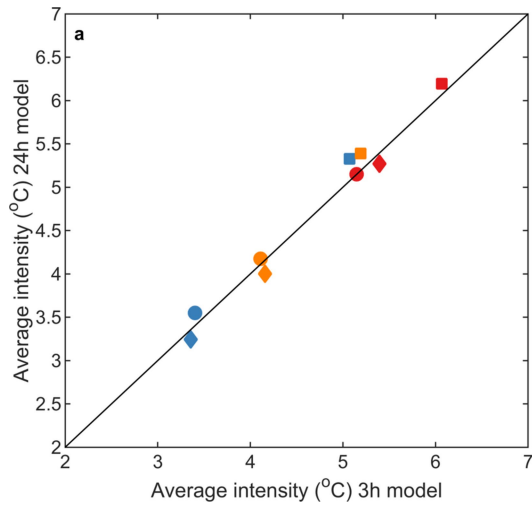
**Extended Data Fig. 8 | Relationship between average lake depth and total heatwave duration from 2070 to 2099.** For each lake thermal region, the relationship between  $\log_{10}$ [mean lake depth (m)] and the total duration of lake heatwave events per year is shown for the end of the twenty-first century

(averaged over all years from 2070 to 2099) under RCP 2.6, RCP 6.0 and RCP 8.5. The relationships between lake depth and the heatwave metrics (square, not significant:  $P > 0.001$ ; circle, significant:  $P < 0.001$ ) were calculated with a generalized additive model (see Methods).



**Extended Data Fig. 9 | Lake thermal responses to climate change.** Here we show the percentage of studied lakes which are projected to experience annual ice cover (a), and experience a permanent heatwave state (b) during the twenty-first century (RCP 8.5). In b, percentages are calculated relative to the number of lakes studied that are projected not to experience annual ice cover by 2070–2099. In c we show a temporally varying (1-year shifting window) 30-year climatological mean, with temperatures plotted as anomalies relative to the historical climatological mean (1970 to 1999). We also demonstrate the

future projections of lake heatwave annual average intensity (d), annual average duration (e) and total duration (f) during the twenty-first century (RCP 8.5) calculated after linearly detrending the lake surface temperature anomalies. All results are based on the average simulations from the lake model driven by the four climate models; the shaded regions represent the standard deviation and the dashed lines represent the range across the lake-climate model ensembles.



**Extended Data Fig. 10 | Comparison of simulated lake heatwaves from two models of different temporal resolution.** Here we compare the simulated lake heatwave intensity (a) and duration (b) by the end of the twenty-first century (averaged over all years from 2070 to 2099) from the FLake model<sup>50,51</sup>

driven at a temporal resolution of 3 h and 24 h for three case study lakes. All results are based on the average simulations from the FLake model, driven by the four climate models.